Estimating Return Intervals for Extreme Climate Conditions Related to Winter Disasters and Livestock Mortality in Mongolia

Masahiko Haraguchi[1,2], Nicole Davi[3,4], Mukund Palat Rao[4,5, 6], Caroline Leland[4], Masataka Watanabe[7], Upmanu Lall[2, 8]

[1] Research Institute for Humanity and Nature, Kyoto, 6038047, Japan
[2] Columbia Water Center, Columbia University, New York, 10027, USA
[3] Department of Environmental Science, William Paterson University, Wayne, NJ, USA
[4] Tree-Ring Laboratory, Lamont-Doherty Earth Observatory of Columbia University, Palisades, NY, USA
[5] Cooperative Programs for the Advancement of Earth System Science, University Corporation for Atmospheric Research, Boulder, CO 80301, USA.
[6] Department of Plant Science, University of California, Davis, CA 95616, United States
[7] Research and Development Initiative, Chuo University, Tokyo, 1128551, Japan
[8] Department of Earth and Environmental Engineering, Columbia University, New York, 10027, USA

Correspondence to: Masahiko Haraguchi (mh2905@columbia.edu)

Abstract. Mass livestock mortality events during severe winters, a phenomenon that Mongolians call dzud, cause the country significant socioeconomic problems. Dzud is an example of a compound event, meaning that multiple climatic and social drivers contribute to the risk of occurrence. Existing studies argue that the frequency and intensity of dzud are rising due to the combined effects of climate change and variability, most notably summer drought and severe winter conditions, on top of socioeconomic dynamics such as overgrazing. Summer droughts are a precondition for dzud because scarce grasses cause malnutrition, which in turn makes livestock more vulnerable to harsh winter conditions. However, these studies typically look at a short time frame (i.e., after 1940~~);~~), and few have investigated either the risk or the recurrence of dzud over a century-scale climate record. This study aims to fill the gaps in technical knowledge about the recurrence probability of dzud by estimating the return ~~levels~~periods of relevant climatic variables: summer drought conditions and winter minimum temperature. We divide the country into three regions (Northwest, Southwest, and East Mongolia) based on the mortality index at the soum (county) level. For droughts, our study uses as a proxy the tree-ring reconstructed Palmer Drought Severity Index (PDSI) for three regions between 1700-2013. For winter severity, our study uses observational data of winter minimum temperature after 1901 while inferring winter minimum temperature in Mongolia from instrumental data in Siberia that extends to the early 19th century. ~~The~~Using a Generalized Extreme Value ~~(i.e., the statistical method to infer the probability of very rare or extreme events) shows~~distribution with time-varying parameters we find that the return ~~levels~~periods of drought conditions are changing over time, with variability increasing for all the regions. Winter severity, however, is ~~constant.~~not changing with time. The ~~median~~ medians of the 100-year return ~~levels~~periods of the winter minimum temperature in Mongolia ~~have been,~~ over the past 300 years~~,~~, are estimated as -26.08°C for the Southwest, -27.99°C for the Northwest, and -25.31°C for the East. ~~This study thus~~The co-occurrence of summer drought and winter severity increases in all the regions in the early 21st century. The analysis suggests that a continued trend in summer drought would lead to increased vulnerability and malnutrition. ~~Here, we link meteorological characteristics to socioeconomic impacts related to livestock populations and draws attention to the need~~Prospects for ~~livestock~~climate index insurance for livestock are discussed.

1 Introduction

1.1 ~~Backgrounds~~Background

Mass livestock mortality induced by dry summers followed by unusually cold and/or snowy winters, known as dzud, causes problems for pastoral herding and the economy in Mongolia.[1] A total of 20 million livestock died of climate extremes from 2000-2002, and 2009-2010 (Rao et al., 2015). In the 2009-2010 dzud alone, approximately 20% of the country's livestock population died, ~~which affected~~affecting 769,000 people, 28% of the population in Mongolia (Middleton et al., 2015) . Dzud is a compound hazard (Field, 2012), encompassing drought, heavy snowfall, extreme cold and windstorms. Dzud can cause mass livestock mortality, which leads to severe socioeconomic consequences such as unemployment, poverty, and mass migration from rural to urban areas (Dagvadorj et al., 2009; Kakinuma et al., 2019). The causes of dzud are complex. Increased population of livestock along with other land use changes such as urbanization and mining are viewed as a major cause of the decline in pasture quality in the region (Bat-Oyun et al., 2016; Berger et al., 2013; Hilker et al., 2014). ~~Along with~~ Other socio-economic factors, such as overgrazing, livestock mortality is caused and exacerbated by the following climate factors: summer drought, heavy snow, and high winds in concurrence with extreme cold winter temperature (Morinaga et al., 2003)~~.~~are also implicated. Livestock mortality is strongly associated with winter (November – February) temperatures and prior summer (July – September) droughts (Rao et al., 2015) and precipitation (Tachiiri et al., 2008; Rao et al., 2015). For example, Rao et al. (2015) showed that ~~the~~a model based on winter temperature, summer drought, summer precipitation, and summer potential evapotranspiration explains 48.4% of the entire variability of mortality. Extreme cold temperature as well as exposure to storms or high winds cause livestock to freeze to death while heavy snow, ice or drought, prevent livestock from grazing and accessing fodder, which results in weakening immune system response and starvation (Begzsuren et al., 2004; Fernandez-Gimenez et al., 2012; Morinaga et al., 2003; Rao et al., 2015)~~.~~ . In addition to extreme winter temperature and snowfall, summer drought is an important driver because droughts deteriorate grazing and prevent livestock from surviving during severe winters (Begzsuren et al., 2004; Rao et al., 2015; Tachiiri et al., 2008). For example, the climate factors that contributed to the dzud in 1999-2002 and 2009-2010 were summer drought followed by extreme cold and snowfall in winter (Field, 2012). In this case, summer drought is regarded as a preconditioning factor for the dzud as a compound event (Zscheischler et al., 2020).

[1] Dzud is Russian way of notation, and it is locally written as "zud" in Mongolia.

Understanding mechanisms and impacts of dzud and climate extremes has wider implications for sustainability in rangelands, which account for 50% of Earth's land surface, where 40% of the world's populations reside (Fernandez-Gimenez et al., 2012; Reynolds et al., 2007). A better understanding of the climate drivers of dzud and extreme events is also critical for preventive and responsive measures, such as weather index insurance. Weather index insurance recently became widely available, and its indemnities are paid based on realizations of a weather index such as rainfall and temperature that are expected to be highly correlated with actual losses, rather than on actual losses experienced by the policyholder (Barnett and Mahul, 2007). The advantage of index insurance is that the pre-determined index cannot be manipulated by the third parties. Payment is faster than loss-based insurance because payment will be made once the predetermined index exceeds the threshold. In contrast, for loss-based insurance, an insurance company must assess losses before making payment, which requires labor and time. The lower transaction costs of index insurance can also make it a more affordable product for the purchaser and thus a more viable offering for the insurance provider. The index-based livestock insurance program (IBLIP) was institutionalized in 2014 to respond to the extreme climate disasters by the Government of Mongolia with help from the World Bank (Skees and Enkh-Amgalan, 2002; Mahul et al., 2015; Mahul and Skees, 2007).

Hessl et al. (2018)~~Few studies have performed risk analysis~~ analyzed variabilities of ~~dzud~~drought in Mongolia using long-term climate data. ~~One reason for this is~~Such studies are still limited by the fact that there are few long-term instrumental records of climate in the region, and the records that do exist are often not continuous and contain missing data. Though historical documents record the occurrence of dzud from the 19th century, changes in climate in Mongolia have been observed in instrumental records only since 1940 (Batima et al., 2005). ~~Additionally~~Some studies ~~concluded~~reported that the frequency of dzud has increased ~~since~~, such as after 1950 (Fernandez-Gimenez et al., 2012; Middleton et al., 2015) or after 2000 (Munkhjargal et al., 2020) ~~and~~. Furthermore, another study concluded that it is expected to increase with future climatic changes (Bayasgalan et al., 2009)~~.~~ using Coupled Model Intercomparison Project's climate models. Natsagdorj (2001) shows that the trends of drought and the dzud index, estimated by normalized monthly temperature and precipitation, are increasing. However, these studies are based on observational data of dzud, which are available only from about 1940. It is critical to extend the time horizon in order to improve the reliability of the return period estimation of catastrophic dzud~~.~~, and of the assertions of secular changes in the causal climate variables. Long-term climate proxies, such as tree rings, have the potential to do so by deriving recurrence periods of dzud and climate extremes, especially to improve index insurance products (Bell et al., 2013). Yet, one of the challenges of improving the reliability of recurrence estimations is the lack of scientific understanding of the historical trends of past climate events due to the short meteorological record (Mahul and Stutley, 2010; Mcsharry, 2014; Rao et al., 2015).

To improve risk analysis of dzud, the investigation of extreme distributions of climate extremes is critical. D'arrigo et al. (2001) inferred using millennial length tree-ring data that temperatures in Mongolia in the late 1990s and early 2000s were ~~extraordinarily.~~extraordinary. Based on well-calibrated and verified millennial-length tree-ring reconstruction of summer temperatures, Davi et al. (2015) and Davi et al. (2021) show that the recent warming trend since the 1990s is anomalous in the long-term context in Mongolia. In addition, Davi et al. (2010) conducted spectral analysis to discover the periodicity of droughts in Mongolia by using tree-ring based reconstructed Palmer Drought Severity Index (PDSI). However, these studies do not estimate probability distributions of extreme climatic events or improve the reliability of the estimation of return periods of dzud for risk analysis. Here, we use the term "risk analysis" to refer to the analysis of the probability of an extreme event whose consequences could be substantial (Rootzén and Katz, 2013), but not the analysis where risk refers to the combination of the probability of an event and its associated expected losses.

1.2 Objectives of the study

The objective of this study is to conduct risk analysis for the climatic variables that cause dzud, namely summer drought followed by extreme cold temperature and snowfall, in Mongolia while attempting to improve the reliability of the return period estimation of dzud utilizing tree-ring proxies and historical data on climatic variables. The study also explores the implications of the risk analysis and return period estimation for index insurance using tree-ring data. To address these objectives, we posed the following research question:

- ***How can the reliability of the return period estimation of climate extremes be improved?***

There are two important climatic variables to predict dzud: summer drought conditions and winter temperatures (Lall et al., 2016; Rao et al., 2015). Notably, this study estimates return periods of extreme drought conditions, by using tree-ring based reconstructed PDSI from the Monsoon Asia Drought Atlas or MADA (Cook et al., 2010). It also estimates return periods of extreme cold temperatures in Mongolia. Since temperature data in Mongolia is only available from the early- to-mid 20th century, we simulate them from meteorological data in neighboring Siberia, which has records that extend back to the late 1800s, through a statistical model presented here. Tree-ring based temperature reconstructions in the region are typically limited to the summer growing season and do not capture winter temperatures.

In Mongolia, the term "dzud" refers to high livestock mortality (Fernandez-Gimenez et al., 2012; Morinaga et al., 2003), however, we use climate variables to determine risk rather than mortality because mortality rate assumes that the size of the population does not matter. In fact, changes in livestock populations also matter since they can also be related to changes in socio-economic factors, such as shortage of food supply, which can be related to non-climate factors. Other socio-economic factors also determine livestock herding loss, including the total number of animals and the density per square kilometer. These numbers drastically increased after a transition to private ownership in 1990s (Douglas A. Johnson, 2006; Rao et al., 2015; Reading et al., 2006). The increased livestock population results in overgrazing and degradation of the grassland, which resulted in a decrease in the grassland carrying capacity and a high mortality rate (Bat-Oyun et al., 2016; Berger et al., 2013; Hilker et al., 2014; Liu et al., 2013).

In order to estimate a return ~~level~~period of an extreme climate event, extreme value theory (EVT) ~~can be~~is useful (Cheng et al., 2014; Katz et al., 2002). There are ongoing debates about which methods are most suitable for estimating extremes, such as the return period and expected number of exceedance (Read and Vogel, 2015; Rootzén and Katz, 2013; Salas and Obeysekera, 2014). EVT informs us how to extrapolate a rare event which has not been experienced for a long time from existing observational data with a short record. EVT is a widely used method for estimating the probability of extreme hydroclimatic events (Katz, 2010; Leonard et al., 2014; Slater et al., 2021), such as floods (Prosdocimi et al., 2015; Willner et al., 2018) (Willner et al., 2018), precipitation (Gao et al., 2018; Minářová et al., 2017), and compound events (Leonard et al., 2014)~~This enables~~. EVT helps us to formulate a risk management strategy by deriving a distribution of extreme climate events and estimating a possible extreme value for the ~~future.~~future's preparedness. There are two main approaches in EVT: The block maximum approach and the threshold approach, which will be described in Data and Methodology. The objectives of this study were to;

- **1. Estimate return periods of extreme drought conditions by using reconstructed PDSI ~~based on extreme value theories.~~.**
- **2. Estimate return periods of extreme cold temperatures in Mongolia by using long instrumental data from Siberia.**

Conventionally, ~~in estimating return periods,~~ a stationarity process is assumed~~.~~ to estimate return periods,. Here, we consider the extension of the record by explicit dependence on climate proxies. ~~Of course, this gives us a stationary return period, which is useful for risk assessment and writing a parametric insurance policy. However, we also~~We examine how the return periods may change over time due to slowly and systematically changing climate conditions, persistence in the PDSI, or other climate records. Exploring the nonstationary approach to return period and risk opens "many opportunities" (Salas & Obeysekera, 2014). This has the advantage of reducing the bias in the near-term projection, assessment of the return period, and recurrence interval associated with the event. ~~Given this information, either the parametric insurance could be repriced up or down, or preparatory actions could be undertaken.~~

~~The study~~We also ~~explores~~explore the utility of using long-term climate proxies in the context of index insurance. In general, the index used for index insurance must be scientifically objective and easily measurable. ~~Though~~ The Index-Based Livestock Insurance Program (IBLIP) in Mongolia uses mortality rate as the index~~, this~~. Our study ~~will explore if~~provides insights into the long term variations in the mortality rate due to climate ~~proxies have the potential to improve~~with the ~~design~~goal of reducing the ~~IBLIP~~bias and the variance of the estimates of the probability of the index used, by identifying the trend, and using a longer record, respectively.

2 Data and Methodology

2.1 Data and Preliminary Analysis

2.2.1 Tree-ring Reconstructed PDSI

Data

PDSI is a standardized index that ranges from -10 (dry) and +10 (wet) based on a water balance model, accounting for precipitation, evaporation, and soil moisture storage (Cook et al., 2010; Dai et al., 2004; Palmer, 1965). In this study, tree-ring reconstructed PDSI values from 1700 to 2013 are taken from Monsoon Asia Drought Atlas (MADA) (Cook et al., 2010). MADA is a seasonally resolved gridded spatial reconstruction of drought and pluvials in monsoon Asia over the last 700 years, derived from a network of tree-ring chronologies (Cook et al., 2010). ~~The benefit of using the three regional clusters is to capture smaller-scale regional details of known droughts because it is based only on the chronologies identified from the principal component analysis .~~ The MADA can also reveal the occurrence and severity of previously unknown monsoon droughts (Cook et al., 2010). We consider three regions (Northwest, Southwest, and East Mongolia) in Mongolia, as in Figure 1, based on clusters proposed by the previous studies (Kaheil and Lall, 2011; Lall et al., 2016)~~Kaheil and Lall (Figure 1).~~. These spatial clusters are based on the mortality data at the soum (county) level from 1972 to 2010, using hierarchical clustering (Johnson, 1967), which were adjusted with the spatial patterns of the Mongolian topography, climate zones, and mean precipitation in growing seasons. It is reasonable to use these clusters because the objective of the study is to improve risk analysis of Dzud and mortality of livestock in Mongolia.

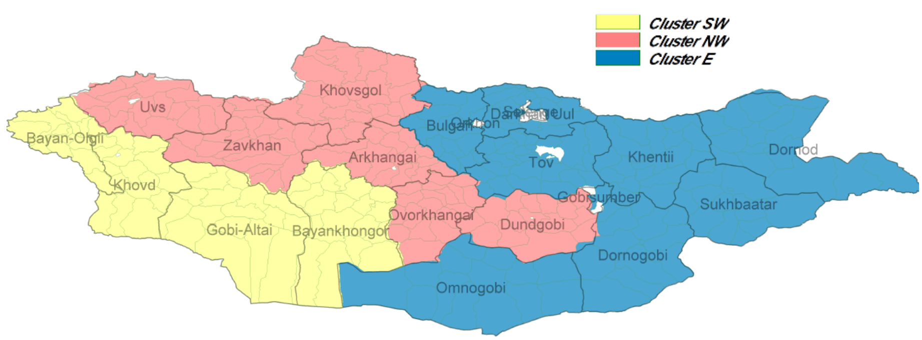

Figure 1: Spatial Clusters of Mortality Index based on 1972-2010 soum level mortality indices. Source: Lall and Kaheil (2011).

Preliminary Analysis

The correlation in PDSI values from 1700 to 2013 between three clusters is shown in Table 1~~Table 1~~. The Mann-Kendall trend test is used to examine the trends of the PDSI data (Kendall, 1948; Mann, 1945). The Mann-Kendall test shows that there are no monotonic trends in the PDSI data for all clusters (Table 1~~Table 1~~). Yet, times series of tree-ring reconstructed PDSI by clusters show that there is significant centennial- scale variability, which is important to consider since they suggest that there are persistent regimes that can last for decades to ~~century~~centennial time scales (Figure 2~~Figure 2~~ (a)-(c)). Though these may occur randomly or reflect systematic cyclical behavior, their consideration in a risk management strategy is critical.

Table 1: ~~Correlations~~Correlation coefficients of PDSI values from 1700 to 2013 between the three clusters

	Mann-Kendall value~~Pearson Correlation Coefficients~~	Pearson Correlation Coefficients~~Mann-Kendall value~~
Southwest	0.0004	-
East	0.0002	-
Northeast	-0.0026	-
Southwest and Northwest	~~0.78~~ -	0.~~0004~~78
Southwest and East	~~0.50~~ -	0.~~0002~~50
Northwest and East	~~0.69~~ -	~~-~~0.~~0026~~69

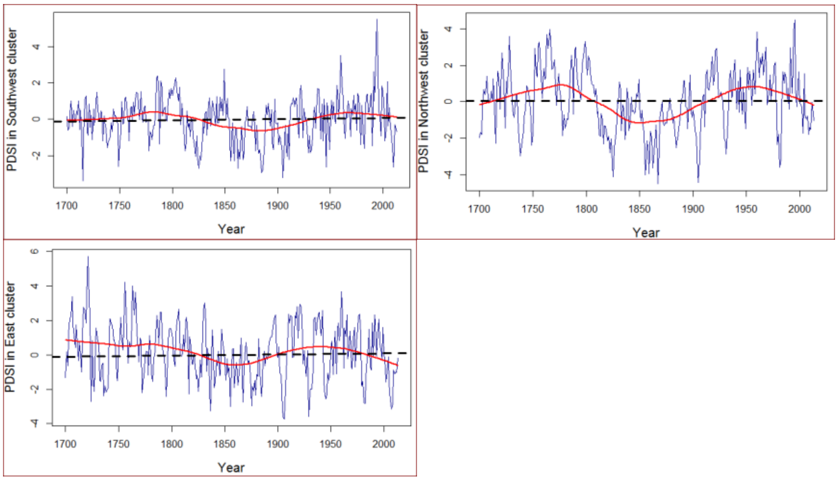
PDSI in Southwest cluster
PDSI in Northwest cluster
PDSI in East cluster
Year

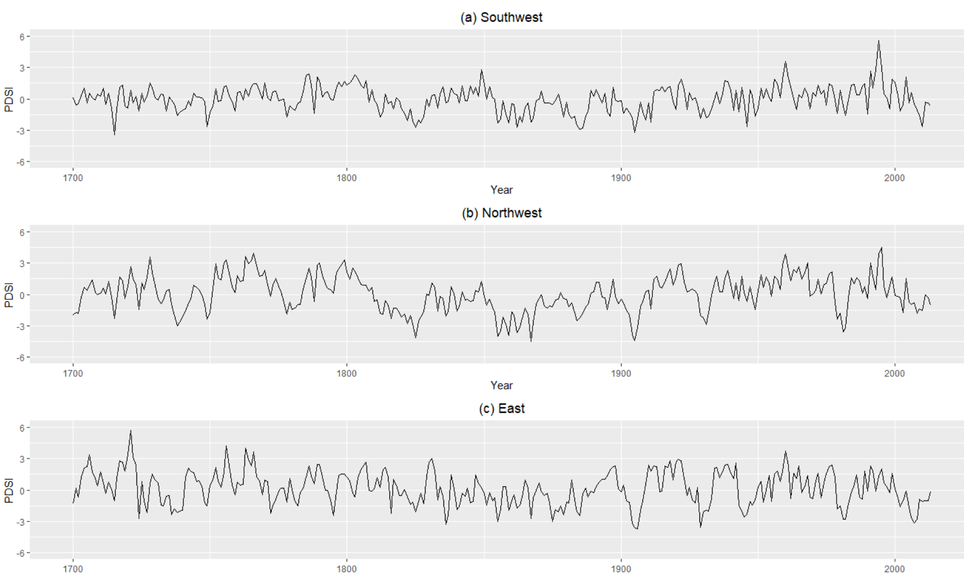
(a) Southwest
(b) Northwest
(c) East
PDSI
Year

Figure 2: Time series of tree-ring reconstructed PDSI in (a) the Southwest, (b) the Northwest, and (c) ~~East clusters . The horizontal line represents the estimated line of the regression of PDSI on year, and the red curve represents a lowess smooth of the data.~~the East clusters.

The autocorrelation function (ACF) and Partial ACF of all the regions show that there are significant autocorrelations in the PDSI data in all clusters (in Figure S1 and S2). The development of a time series simulation model that uses these long lead correlations would help inform the risk analysis associated with the persistent regimes identified earlier. ~~Thus,~~ Autoregressive~~-~~ Integrated Moving ~~-~~Average (~~ARMA~~ARIMA) models with different orders ~~are~~were evaluated based on the Bayesian Information Criterion (BIC), which can account for fitting errors for the Bayesian conditional mechanism of models. Please note that the BIC is standard information-theoretic criteria whose relative magnitudes allow one to choose one model over another (Akaike, 1979; Burnham and Anderson, 2004). The order of the best ARIMA models in each cluster is (3,0,0) for the Southwest, (1,0,2) for the Northwest, and (1,0,0) for the East. These ARIMA models will be used later to forecast the effective return periods of droughts.

2.2.2 Climate variables

Models that use climate variables as covariates are explored for developing a nonstationary risk model. These data are summarized in Table 2~~Table 2~~. We use high-resolution gridded datasets at Climate Research Unit (CRU) at University of East Anglia for monthly temperature, and summer (May-August) and winter (November-February) precipitation for the three clusters (Harris et al., 2014). All the gridded points within each cluster are averaged. We also used average monthly temperature data from instrumental records in Siberia, including Irkutsk (1882-2011), Minusinsk (1886- 2011), and Ulan Ude (1895-1989). We also use the Arctic Oscillation (AO) index, which comes from two sources: the Joint Institute for the Study of the Atmosphere and Ocean (JISAO) and the National Oceanic and Atmospheric Administration (NOAA). The two records were ~~scaled to be~~ merged into one record (e.g. Kaheil and Lall, 2011)). The AO index is closely associated with summer and winter climates in East Asia (He et al., 2017). In particular, the negative phase of AO is associated with more frequent cold air outbreaks in East Asia, including Mongolia (Cohen et al., 2010; He et al., 2017; Yu et al., 2015). Finally, please note that though dry conditions of PDSI is negative, all the analyzed PDSI values below are presented in reversed values because the used R package, extReme (Gilleland and Katz, 2016), will capture the maximum values.

Formatted: Font: Not Bold

Table 2: List of data analyzed in this study

	Types	Periods	Regions	Source
Tree-ring reconstructed PDSI data	534 grid point reconstructions on a 2.5x2.5° grid	1700 ~~–~~- 2013	Southwest, Northwest, And East Mongolia	Cook et al (2010)

Monthly temperature	High-resolution gridded climate datasets (0.5 x 0.5-degree resolution)	1901 - 2014	Southwest, Northwest, And East Mongolia	World Meteorological Organization
Monthly minimum temperature	High-resolution gridded climate datasets (0.5 x 0.5-degree resolution)	1901 ~~–~~- 2014	Southwest, Northwest, And East Mongolia	World Meteorological Organization
Monthly temperature in Irkutsk, Siberia	Instrumental climate data	Sept. 1820 - June 2016	- 52.27N, 104.32E. 469.0m (prob: 490m) - WMO station code: 30710 IRKUTSK	GHCN-M v3.3.0.20160703
Monthly temperature in Ulan-UDE, Siberia	Instrumental climate data	Aug. ~~1886~~1866 - Dec. 1990	- 51.83N, 107.60E, 515.0m (prob: 641m) - WMO station code: 30823 ULAN-UDE	GHCN-M v3.3.0.20160703
Monthly temperature in Minusinsk, Siberia	Instrumental data	Jan. 1886 - June 2016.	- 53.70N, 91.70E, 254.0m (prob: 369m) - WMO station code: 29866 MINUSINSK	GHCN-M v3.3.0.20160703
Summer and Winter precipitation	High-resolution gridded datasets (0.5 x 0.5-degree resolution)	1901 ~~–~~- 2014	Southwest, Northwest, And East Mongolia	CRU

AO~~—~~-Index	1903 - 2010	Joint Institute for the Study of the Atmosphere and Ocean (JISAO) and National Oceanic and Atmospheric Administration (NOAA).

2.2 Methodology

Extreme Value Analysis (EVA) is utilized in this study. In EVA, the distribution of many variables can be stabilized so that their extreme values asymptotically follow specific distribution functions (Coles et al., 2001). There are two primary ways to analyze extreme data. The first approach, the so- called block maxima approach, reduces the data by taking maxima of long blocks data, such as annual maxima (Coles et al., 2001). The Generalized Extreme Value (GEV) distribution function is ~~fitted~~fit to maxima of block data, as given by

$$\mathrm{G}(z) = \exp\left[-\left\{1+\varepsilon\left(\frac{z-\mu}{\sigma}\right)\right\}_{+}^{-1/\varepsilon}\right] \quad (1)[2]$$

where, $y_+ = \max\{y, 0\}, \sigma > 0, and -\infty < \mu, \varepsilon < \infty.$

Equation (1) ~~enclose~~covers three types of distribution ~~function~~functions depending on the sign of the shape parameter ε. The Fréchet distribution function is for ~~ε>0~~ ε>0 while the upper bounded Weibull distribution function is for ε<0(Gilleland and Katz, 2016). The Gumbel type is obtained in the limit as ε→0, which results in

$$\mathrm{G}(z) = \exp\left[-exp\left[-\left\{\frac{z-\mu}{\sigma}\right\}\right]\right], -\infty < z < \infty \quad (2)$$

The second approach, the so-called threshold excess approach, is to analyze excesses over a high threshold (Coles et al., 2001). The Generalized Pareto Distribution (GPD) has a theoretical justification for fitting to the threshold excess approach (Gilleland and Katz, 2016), as given by

[2] For mathematical notation, y+ means max (y, 0), meaning that if y is negative, choose zero, otherwise choose y. Then, in equation 1, "+" indicates the same meaning. If the inside of the parentheses is negative, take zero.

$$H(x) = 1 - \left[1 + \varepsilon\left(\frac{x-\mu}{\sigma_\mu}\right)\right]_{+}^{-1/\varepsilon} \quad (3)$$

where μ is a high threshold, x> μ, scale parameter σ_μ>0 and shape parameter $-\infty < \varepsilon < \infty$. The shape parameter ε determines three types of distribution functions: heavy-tailed Pareto when ε>0, upper bounded Beta when ε<0, and the exponential is obtained by taking the limit as $\varepsilon \to 0$, which gives

$$H(x) = 1 - e^{-(x-\mu)/\sigma} \quad (4)$$

The extreme value models can be applied in the presence of temporal dependence (Coles et al., 2001), as given below:

$$Zt \sim \text{GEV}\ (\mu(t), \sigma(t), \varepsilon(t)) \quad (5)$$

~~Where~~

where, $\mu(t) = \alpha_0 + \alpha_1 t + \alpha_2 t^2 + .. + \alpha_n t^n$

$$\sigma(t) = \exp\ (\beta_0 + \beta_1 t + .. + \beta_n t^n)$$

$$\varepsilon(t) = \begin{cases} \varepsilon_0, & t \le t_0 \\ \varepsilon_1, & t > t_0 \end{cases}$$

By examining the times series of the PDSI values and winter minimum temperature, we can enhance the understanding of how return periods of droughts, and extreme cold weather have changed over time. The best GEV and GPD models are selected based on Maximum Likelihood Estimation (MLE) and BIC (Katz, 2013). Also, ~~it is examined in~~ diagnostic plots were used to assess whether the best GEV and GPD models are reasonably ~~fit~~fits to the distributions ~~or not~~.

3 Main Results and Discussion

3.1 Return Periods of Droughts Using Tree-ring Reconstructed PDSI data

~~In this section, to find the best model to predict a drought condition with the extended time,~~ GEV and GP distributions are fit to the tree-ring reconstructed PDSI values for approximately 300 years, from 1700 to 2013. ~~Specifically, in order to estimate return periods of extreme drought conditions, tree-ring based reconstructed PDSI and extreme value theories are used. Block maximum approach by using GEV distributions and threshold approach by using GPDs will be used while checking the stationarity of the data. If it is not stationary, the non-stationary extreme value technique will be used.~~ Stationarity is assessed through the comparison of the BIC applied to a set of candidate models formualted using equation 5, with terms that include time or not.

The procedure is implemented as follows:

1. Fit GEV distributions to the tree-ring reconstructed PDSI values, allowing for non-stationarity by making μ, σ, and/ or ε a function of time.

2. Fit GEV distributions to the tree-ring reconstructed PDSI values using climate variables (AO index, summer precipitation, snow, and minimum temperatures).

3. Evaluate models based on BIC.

4. Using the best GEV model, return periods are estimated.

5. The above procedure is repeated for GPDs fit to the tree-ring reconstructed PDSI values.

3.1.1 Fitting GEV to the Tree-Ring Reconstructed PDSI for Return Period Estimation

We construct two types of models: (1) stationary and nonstationary extreme value models, and (2) nonstationary models using climatic variables as covariates. First, we consider polynomial models in time of the order of 0 to 2 for both the location and scale parameters of the GEV distribution, resulting in seven models to be tested, including the stationary model, for each region. In addition, autoregressive (AR) models are examined. The models are evaluated based on the BIC (Table 3~~Table 3~~). The best GEV models and its maximum likelihood estimates (MLE) with 95% confidence intervals are as follows (Table 3~~Table 3~~, Figure 3~~Figure 3~~):

- Southwest: the model with a constant in the location parameter and temporally linear model in the scale parameter; the AR (3) model:

  $\mu = -0.42;\ \sigma = \exp\,(0.95 + 0.002t\cancel{;});\ \varepsilon = -0.23.\ (\mathrm{BIC} = 1045).$

  $\mu = -0.39 + 0.36PDSI_{t-3};\ \sigma = 1.19\ ;\ \varepsilon = -0.29.\ (\mathrm{BIC} = 1005).$

- Northwest: the model with a constant both in the location and scale parameters; AR (3) model:

  $\mu = -0.67;\ \sigma = 1.68;\ \varepsilon = -0.25;(\mathrm{BIC} = 1241).$

  $\mu = -0.57 + 0.50PDSI_{t-3};\ \sigma = 1.47\ ;\ \varepsilon = -0.27.\ (\mathrm{BIC} = 1146).$

- East: the model with a constant both in the location and scale parameters; AR (1) model:

  $\mu = -0.93;\ \sigma = 1.65;\ \varepsilon = -0.31;(\mathrm{BIC} = 1212).$

  $\mu = -0.55 + 0.62PDSI_{t-1};\ \sigma = 1.25\ ;\ \varepsilon = -0.22.\ (\mathrm{BIC} = 1064).$

Table 3: BIC values for stationary and non-stationary GEV models fitted to the tree-ring reconstructed PDSI values.

				Southwest	Northwest	East
Stationary model				1049	**1241**	**1212**
~~BIC~~	~~Stationary model~~	Non-stationary model	L = 1, S = 0	1053	1246	1248

Formatted: Font: Not Bold

Formatted: Font: Not Bold

Formatted: Font: Not Bold

Deleted Cells

Deleted Cells

Inserted Cells

Inserted Cells

Inserted Cells

~~el~~			~~ARmodel~~ L=0,S=1	1045	1246	1218				
	~~L=1,S=0~~	~~L=0,S=1~~	L=1,S=1	1048~~L=2,S=1~~	~~L=1,S=2~~1252	~~L=2,S=2~~ 1216				
			L=2,S=1	1050	1242	1217				
~~Southwest~~			L=1,S=2	1053	1252~~1045~~	1222 ~~1048~~	~~1050~~	~~1053~~	~~1056~~	~~1005 AR(~~

Deleted Cells
Deleted Cells
Deleted Cells
Deleted Cells

Deleted Cells
Deleted Cells
Deleted Cells
Deleted Cells

	~~1049~~ L = 2, S = 2	1056	1248	1222	~~3)~~
AR model~~Northwest~~	~~1241~~	1005 ~~1246~~	~~1 2 4 6~~ ~~1 2 5 2~~ ~~1 2 4 2~~ ~~1 2 5 2~~ ~~1 2 4 8~~	1146~~AR(3)~~	1064
~~East~~	~~1212~~	AR(3)~~1248~~	AR(3) ~~1218~~ ~~1 2 1 6~~ ~~1 2 1 7~~ ~~1 2 2 2~~ ~~1 2 2 2~~	~~1064~~AR(1)	

Note: L stands for the location parameters, S stands for the scale parameters. 0 means a constant in the parameter, 1 is temporally linear, and 2 is temporally quadratic for each parameter.

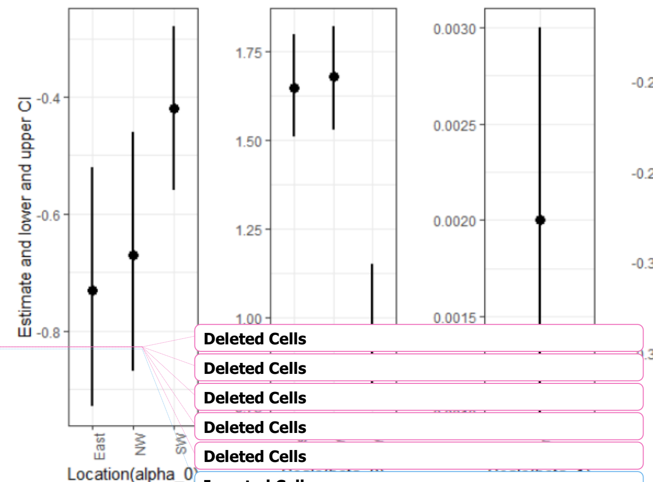

Deleted Cells
Deleted Cells
Deleted Cells
Deleted Cells
Deleted Cells
Inserted Cells
Deleted Cells
Deleted Cells
Deleted Cells
Deleted Cells
Deleted Cells

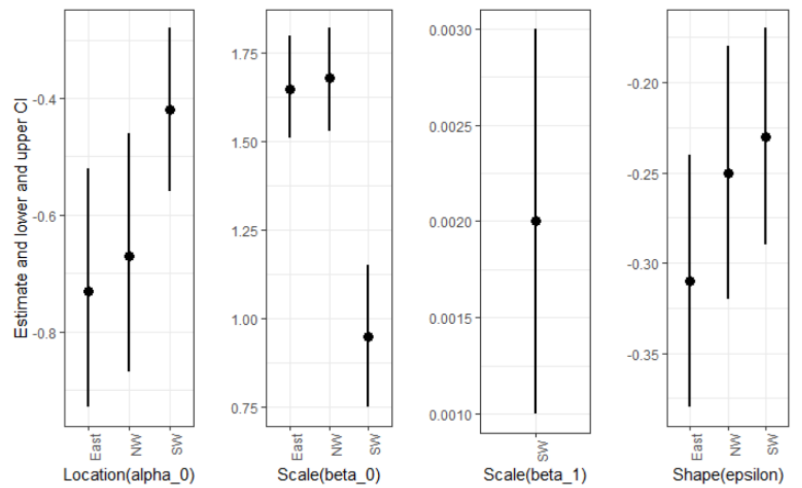

Figure 3: 95% Confidence intervals of parameters based on the normal approximation for each parameter. Also numerical values are listed in Table S.1.

These results suggest that in the long run, a stationary model for PDSI in Mongolia may be appropriate. Only the Southwest has nonstationarity in the scale parameter~~, and~~. This nonstationarity in the scale parameter for the Southwest, with a mean coefficient of 0.002 relative to the constant value of 0.95, means that over 100 years the variability could increase from 0.9 to 1.05. If we take 0.9 to be a mid-period estimate, this would be rather a modest change. This could be a real feature or an artifact of the non-constant reconstruction variance from the tree ring reconstruction algorithm.

Next, we estimate parameters of the GEV distribution functions fit to the PDSI values by including other climate variables such as AO index, summer precipitation, snow, and minimum temperatures as covariates from 1903 to 2010. Summer precipitation is a mean of May to August of a previous year, while snow is mean of values from November of a previous year to February of the year~~ (~~. Also, AO index data starts in 1903. Thus, we use data starting 1903 though the data itself exists since 1901~~)~~. The minimum temperature is a minimum value from November of a previous year to October of the year. The GEV models with the lowest BIC for each cluster and MLEs with the 95% confidence intervals are as follows (Table 4~~Table 4~~ and Figure 4~~Figure 4~~):

Formatted: Font: Not Bold

Formatted: Font: Not Bold

- Southwest: *Precipitation* data as a linear covariate in the location parameter:

  $\mu = 3.63 - 0.14Precipitation;\ \sigma = 1.12;\ \varepsilon = -0.21.$ (BIC = 358).

- Northwest: *Precipitation* data as a linear covariate in the location parameter and *snow* data as a linear covariate in the scale parameter.

  $\mu = 6.25 - 0.15Precipitation;\ \sigma = 2.38 - 0.31snow; \varepsilon = -0.07.\,(\mathrm{BIC} = 380).$

- East: *Precipitation* data as a linear covariate in the location parameter.

  $\mu = 5.09 - 0.13Precipitation;\ \sigma = 1.48;\ \varepsilon = -0.24.\,(\mathrm{BIC} = 380).$

In the GEV models, climate variables (precipitation and snow) are important covariates for the extreme values of the PDSI values and improve the model performance (Table 3~~Table 3~~). These climate variables have no inter-year dependence that is significant based on ARIMA, and hence there is no memory in these variables and the best model is stationary model. Consequently, no near-term forecast is feasible.

Formatted: Font: Not Bold

Table 4: BIC values in estimated GEV models fitted to the PDSI values using the climate variables from 1903 to 2010.

		Scale				
Southwest						
		Constant	AO	Snow	Tmin	Precip
Location	Constant	392	397	397	394	391
	Linear trend	390	393	393	394	393
	Quadratic trend	387	390	391	387	390
	AO	397	401	401	397	393
	Snow	397	401	401	398	395
	Tmin	396	401	401	396	395
	Precip	**358**	361	362	362	362
Northwest						
		Constant	AO	Snow	Tmin	Precip
Location	Constant	430	434	433	433	432
	Linear trend	433	437	437	437	436
	Quadratic trend	427	431	431	429	425
	AO	434	438	437	437	437
	Snow	434	438	437	437	437
	Tmin	433	437	437	436	436
	Precip	384	388	**380**	387	387
East						

		Constant	AO	Snow	Tmin	Precip
Location	Constant	439	437	444	443	440
	Linear trend	441	446	445	446	445
	Quadratic trend	440	445	445	445	443
	AO	444	448	448	448	445
	Snow	439	444	442	443	441
	Tmin	444	448	448	448	444
	Precip	**416**	418	418	420	419

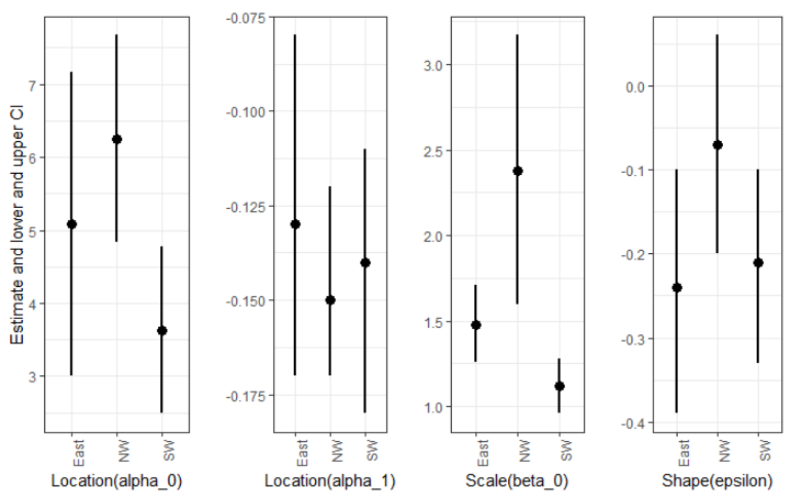

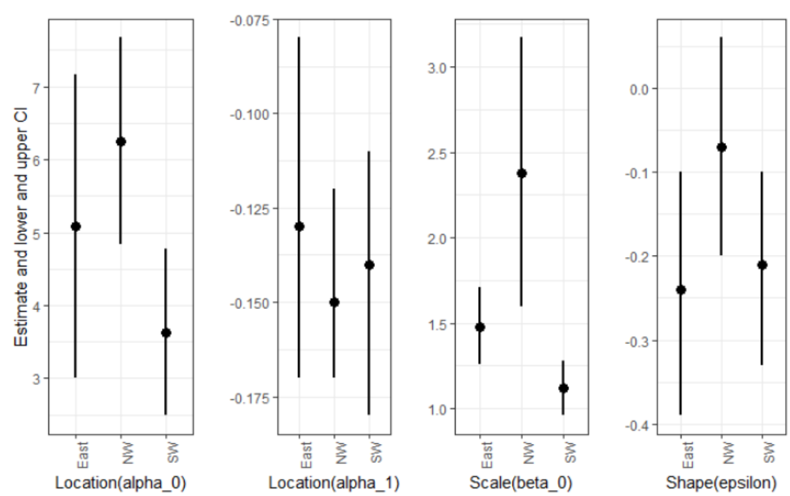

Figure 4: 95% Confidence intervals of parameters, using other climate variables based on the normal approximation. Also numerical values are listed in Table S.2.

The time series of effective return periods of 100-year events for the GEV distribution functions fitted to the PDSI using the climate variables are shown in the Southwest, Northwest, and East from 1903 to 2010 (Figure 5~~Figure 5~~). This shows that variabilities of return periods of 100-year events of the PDSI values become larger over time in all the regions. Before 1940, the variabilities are small possibly because the instrumental data records began in 1940's. Even after 1940's, it also shows that the magnitude of 100-year events has increased in the last half of the data series. A PDSI value of 3 used to be a 100 year event around 1920. Yet, around the beginning of the 21st century, it has increased to be between 4 and 5. However, considerable inter-annual and decadal variability is evident.

Formatted: Font: Not Bold

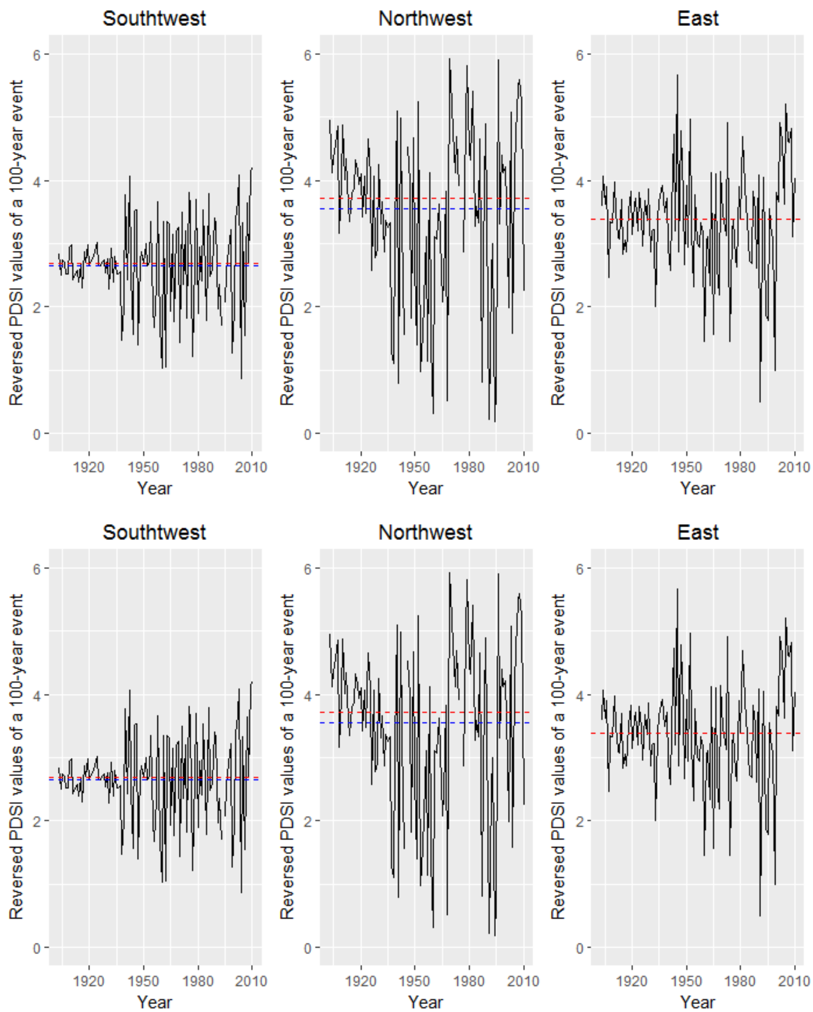

Figure 5: Estimated effective return ~~levels~~periods of a 100-years event from the GEV distribution function fitted the PDSI values in the Southwest over 1903 to 2010 with precipitation data as a linear covariate in the location parameter. Variabilities of return periods of 100-year events of the PDSI values become larger over time in all the

regions. The blue horizontal line is the mean of the effective return ~~levels~~periods while the red one is its median. Please note that the vertical axis is shown by the reversed values of PDSI values, meaning that a positive value is a drought condition.

The relationship between significant climate covariates and reversed reconstructed PDSI values based on the best GEV models for each return period of 10, 50, and 100 years events are shown in Figure 6~~Figure 6~~ and Figure 7~~Figure 7~~. This shows that less precipitation leads to higher reversed reconstructed PDSI values, meaning more likelihood of droughts. Consequently, with this model, future projections of precipitation could be helpful to predict drought severity and frequency.

Formatted: Font: Not Bold

Formatted: Font: Not Bold

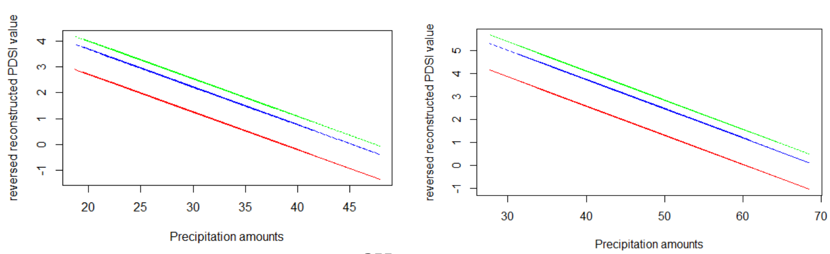

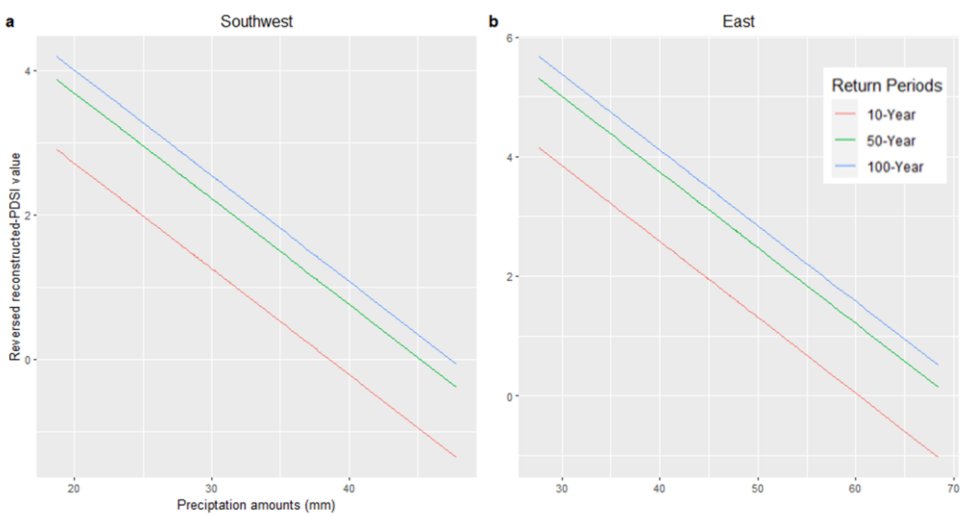

Figure 6: Relationship between precipitation and reversed reconstructed PDSI values in the Southwest (left) and the East (right) based on the best GEV model. Since the PDSI values are reversed, the positive values mean drought conditions. The red, blue and green lines are 10 year, 50 year, and 100 year events. This shows that less precipitation leads to higher reversed reconstructed PDSI values, meaning more likelihood of droughts .

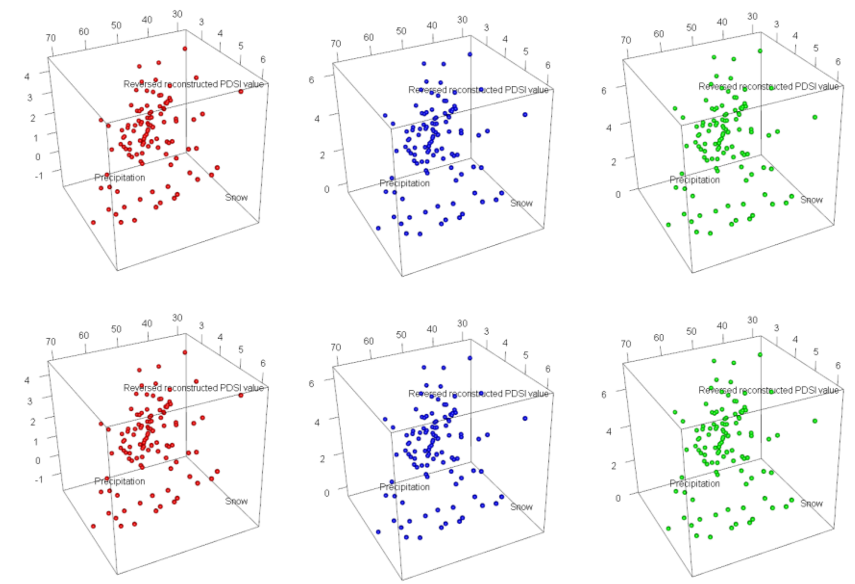

Figure 7: Relationship between precipitation, snow and reversed reconstructed PDSI values in the Northwest based on the best GEV model. Since the PDSI values are reversed, the positive values mean drought conditions. The x axis is precipitation, the y-axis is snow, and the z-axis is reversed reconstructed PDSI values. The ~~right~~left? cube is for 10-year events, the central is for 50-year events, and the right is for 100-year events. Since the best GEV model contains precipitation and snow as covariates, the model for the Northwest is cubic. This shows that less precipitation leads to higher reversed reconstructed PDSI values, meaning more likelihood of droughts.

3.1.2 Fitting GPD to the Tree-Ring Reconstructed PDSI for the Return Periods Estimation

To fit a GPD, a threshold needs to be selected. We selected a threshold of 1.0 (please see the ~~appendix A~~Supplement S1 for the detailed explanation of how we ~~chosen~~chose the threshold). GPDs are fit to the tree-ring reconstructed PDSI values from

1700 C.E. as both stationary and non-stationary models (Table 5~~Table 5~~). The model of stationarity is best in terms of BIC for all clusters.

Table 5: BIC values for non-stationary models in the scale parameters of GPD models fitted to the tree-ring reconstructed PDSI from 1700 for each ~~clusters~~cluster.

~~BIC~~	Constant	Linear in time	Quadratic in time
Southwest	**97.00**	100.30	104.40
Northwest	**184.69**	188.37	188.41
East	**143.49**	145.01	148.25

The likelihood ratio test shows similar results. The likelihood ratio between temporal linear and stationary models shows that the p-value is 0.24. The likelihood ratio test between temporal quadratic and stationarity model shows 0.49 of p-values. Both results show that the subset models do not improve significantly. These results confirm that for PDSI values a stationary model is appropriate.

Being similar to the GEV cases, we analyze the other climate variables after 1903. Table 6~~Table 6~~ shows that the best model of GPD is the one with a constant in the scale parameters in terms of BIC for all clusters. MLEs estimated by the best GPD models are shown in Figure 8~~Figure 8~~. The table shows that for catastrophic droughts, climate variables are not a significant covariate, although the differences in BIC values in the Southwest and Northwest between the ones with constants and with AO index are small. The estimated effective return periods based on these best GPD models are listed in Table 7~~Table 7~~. In Table 7, the difference between the values for 10, 50, and 100 years is slight because the shape parameters estimated from the GEV for each case are negative. This means that the data is negatively skewed and this leads to an implicit upper bound for the process. As a result, each of the quantiles is restricted by that upper bound and ends up quite close to each other.

Table 6: BIC values for different GPD models fitted to the tree-ring reconstructed PDSI values from 1903 with climate variables for all clusters

Predictors in the scale parameters	Constant	AO	Snow	Tmin	Precip
Northwest	**30.21**	31.37	32.16	32.20	31.96
Southwest	**50.38**	50.82	53.00	52.09	52.76
East	**65.49**	68.84	68.62	68.86	67.80

Formatted: Font: Not Bold

Formatted: Font: Not Bold

Formatted: Font: Not Bold

Formatted: Font: Not Bold

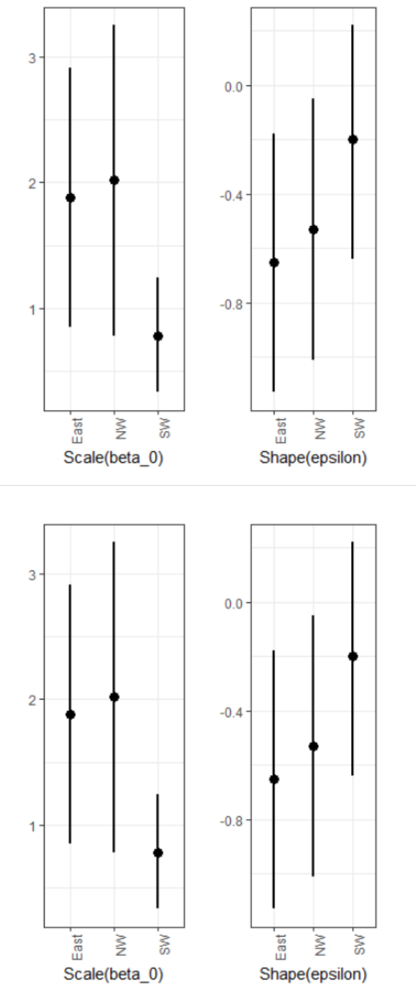

Figure 8: 95% Confidence intervals of parameters, using other climate variables based on the normal approximation. Also numerical values are listed in Table S.3

Table 7: Effective return ~~levels~~periods of 10, 50, and 100 year events of the PDSI values, based on the best GPD models. (Actual PDSI values are negative of these values).

	10 year event	50 year event	100 year event
Southwest	3.82	4.08	4.17
Northwest	4.68	4.75	4.76
East	3.85	3.87	3.87

Results Based on GEV and GPD Models

In this section, we fitted the GEV and GPD distribution functions to the PDSI values. Results are the following:

- ~~All~~ The results show that the PDSI values will follow the distributions with ε<0, namely the Weibull distribution for the GEV models and the upper-bounded Beta distribution for the GPD models. This information can be used to estimate return periods of extreme drought.
- For the Southwest, the non-stationary models performed better if we look at GEV without a threshold. However, with a threshold of 1 for the GPDs, the stationary models perform better than the non-stationary models, which indicate that all trends in reconstructed PDSI values are influenced by small events, not by extreme events; i.e. extreme events are stationary. For both the Northwest and East, stationary models performed better for both the GEV and GPD models.
- Compared to the models with constants in the parameters, the GEV model with the climate variables are better in terms of the BIC value. Therefore, establishing a relationship between drought conditions and climate variables, particularly precipitation and snow, is useful in understanding the dynamics that determine dry conditions. However, compared to the models with constants in the scale parameters, the GPD models with the climate variables don’t lead to the improvement of the model performance~~. Hence, the climate variables are not so useful for understanding the catastrophic dry conditions.~~ in terms of the BIC criteria.
- In terms of BIC, the models of a GPD fitted to tree-ring reconstructed PDSI values show better performance than the GEV models.
- Because of the third point, the effective return periods based on the GEV models change with the climate variables. In contrast, the effective return ~~levels~~periods based on the GPD models are constant: for example, a 100-year event is the PDSI value of -4.17 for the Southwest, -4.76 for the Northwest, and -3.87 for the East. This suggests that while the magnitude of the annual maxima seems to change with the base climate conditions, the frequency of the extreme events beyond a threshold is not affected that much.

3.2 Simulating Annual Minimum Temperature in Mongolia Using Siberia Data

Instrumental winter temperature data in Mongolia is limited before 1950. Also the gridded climate database that cover Mongolia starts after 1901. Thus, we attempt to estimate the Mongolia data from longer records from Siberia, which can get back to 1820. Existing studies suggest the winter temperatures between Mongolia and Siberia are correlated spatially, driven by polar jet dynamics (He et al., 2017; Iijima and Hori, 2018; Munkhjargal et al., 2020). First, winter temperatures in Mongolia will be simulated by using instrumental temperature data from Siberia (in Section 3.2). By using the simulated winter temperature in Mongolia, return periods of extreme cold temperature during winters will be estimated in Section 3.3.

~~Instrumental winter temperature data in Mongolia is limited before 1950. Thus, we attempt to estimate the Mongolia data from longer records from Siberia.~~ The procedure was implemented as follows:

1. Conduct correlation analysis between Siberia and Mongolia data to select which station data are informative for temperature in Mongolia.
2. Impute missing data of instrumental data in Siberia
3. Fit a GEV and GPD to the winter minimum temperature in Mongolia with the Siberia data
4. Simulate winter minimum temperature of Mongolia from Siberia data based on the best GEV model.
5. Calculate effective return periods of 10, 50, and 100 years from the simulated winter minimum temperature of Mongolia.

First, correlation analysis is conducted to see which station data in Siberia is useful for Mongolia data. Temperature data in both Mongolia and Siberia is monthly data. ~~Thus, to remove the seasonality,~~ We use minimum temperature and average temperature during the winter time (October to April~~).~~) to remove the seasonality. We remove the seasonality because if both series data have seasonality (or periodicity), the correlation between them will be high just for that reason. Removing seasonality helps us identify if the anomalies from the periodic behavior are correlated, or namely if they share similar dynamics in effects induced by atmospheric circulation beyond the seasonal cycle. Data are taken for the common periods when all the points have data (i.e. between 1901 – 1990). Irkutsk data alone is used since it alone shows significant correlations between the temperature data in Mongolia and Siberia (Results of Pearson and Spearman correlation coefficients and scatter plots are shown respectively in Table S.4, Figure S.~~5~~8 and Figure S.~~6~~9 in the ~~appendix~~supplement.) We also check the ACF of residuals between data from Irkutsk, Siberia and winter average temperature of each cluster, and find out that there is no significant ACF structures between these data (Figure S.~~7~~10).

Next, we checked the structures of missing data from Irkutsk. Some years are missing all monthly records. We impute Irkutsk's data with pattern matching methods, which is equivalent to k-nearest neighbors, by Gibbs sampling using predictive mean matching method (Van Buuren and Groothuis-Oudshoorn, 2011). Using winter minimum temperature from the Irkutsk data in Siberia ($Tmin_{Irkutsk}$) as a covariate, we fit the Mongolia winter minimum temperature ($Tmin_{mongolia}$) based on the GEV and GPD models.

3.2.1 Fitting GEV to the Winter Minimum Temperature in Mongolia

The results for GEV models based on BIC are shown in Table 8~~Table 8~~. Models with Siberia data both in the location and scale parameter are the lowest BIC for the ~~Southwest and~~ Northwest. For the Southwest and East, the one with Siberia data in the location parameter and constant in the scale parameter shows the lowest BIC (Table 8~~Table 8~~). The best models for each region are shown in Figure 9~~Figure 9~~ and in the following:

$$\mathrm{H}(Tmin_{mongolia}) = 1 - \left[1 + \varepsilon\left(\frac{Tmin_{mongolia} - \mu}{\sigma_{\mu}}\right)\right]_{+}^{-1/\varepsilon} \quad (6)$$

$$\mathrm{Zt} \sim \mathrm{GEV}\ (\mu(t), \sigma(t), \varepsilon(t)) \quad (7)$$

where

$\mu(Tmin_{Irkutsk}) = \beta_0 + \beta_1 * Tmin_{Irkutsk}$

$\sigma(Tmin_{Irkutsk}) = \exp\ (\beta_3 + \beta_4 * Tmin_{Irkutsk})$

$\varepsilon(t) = \begin{cases} \varepsilon_0, & t \le t_0 \\ \varepsilon_1, & t > t_0 \end{cases}$

Southwest: $\mu = 11.80 + 0.39 Tmin_{Irkutsk}$; $\sigma = 1.90$; $\varepsilon = -0.25$.

Northwest: $\mu = 12.67 + 0.52 Tmin_{Irkutsk}$; $\sigma = exp(0.35 + 0.06 Tmin_{Irkutsk})$; $\varepsilon = -0.18$.

East: $\mu = 10.20 + 0.48 Tmin_{Irkutsk}$; $\sigma = 1.40$; $\varepsilon = -0.38$.

Table 8: BIC values for GEV models using Irkutsk data for 3 clusters

	Stationary	Location~~=~~ = $Tmin_{Irkutsk}$, scale =1	Location~~=~~ = 1, scale = $Tmin_{Irkutsk}$	Location~~=~~ = $Tmin_{Irkutsk}$, scale = $Tmin_{Irkutsk}$
Southwest	527.40	**494.45**	528.98	497.40
Northwest	537.04	467.87	532.89	**467.74**
East	495.48	**403.36**	846.02	901.64

Formatted: Font: Not Bold

Formatted: Font: Not Bold

Formatted: Font: Not Bold

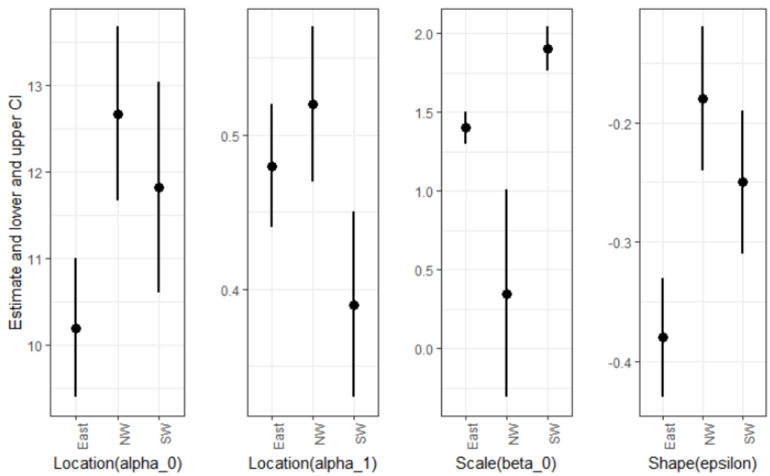
Estimate and lower and upper CI
Location(alpha_0)
Location(alpha_1)
Scale(beta_0)
Shape(epsilon)
East
NW
SW

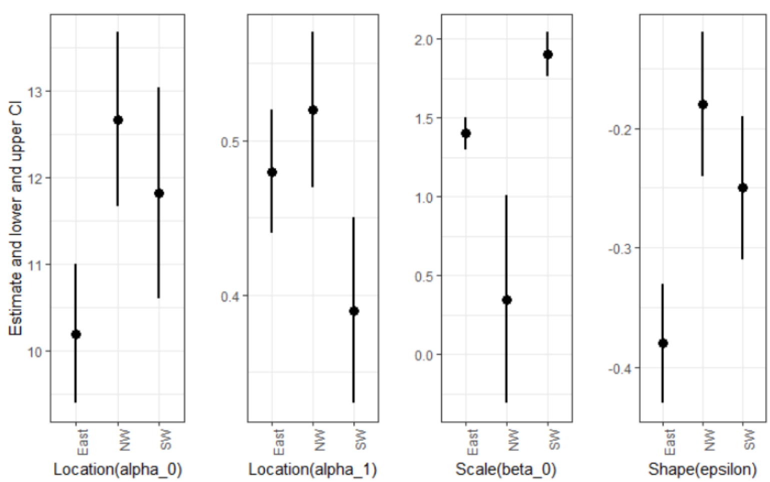
Estimate and lower and upper CI
Location(alpha_0)
Location(alpha_1)
Scale(beta_0)
Shape(epsilon)
East
NW
SW

Figure 9: **Estimated parameters based on the best GEV model fitted to the winter minimum temperature in Southwest using Irkutsk data. Numerical values are listed in Table S.5.**

3.2.2 Fitting GPD to the Winter Minimum Temperature in Mongolia

For GPD, we select ~~20 (-20~~23 (-23 degrees in reality) as a threshold~~.~~ (Please see Section S.1, Figure S6 and Figure S.7 in Supplemental regarding how the thresholds were selected). In this case, the one with the Irkutsk's data in the scale parameter has the lowest BICs for all clusters as Table 9~~Table 9~~ shows.

Formatted: Font: Not Bold

Table 9: BIC values of GPD models using Irkutsk data for 3 clusters

	Stationary	Scale = $Tmin_{Irkutsk}$
Southwest	~~242.00~~54.78	**~~236.00~~53.26**
Northwest	~~503.92~~282.30	**~~479.89~~270.72**
East	~~203.52~~31.38	**~~180.15~~28.49**

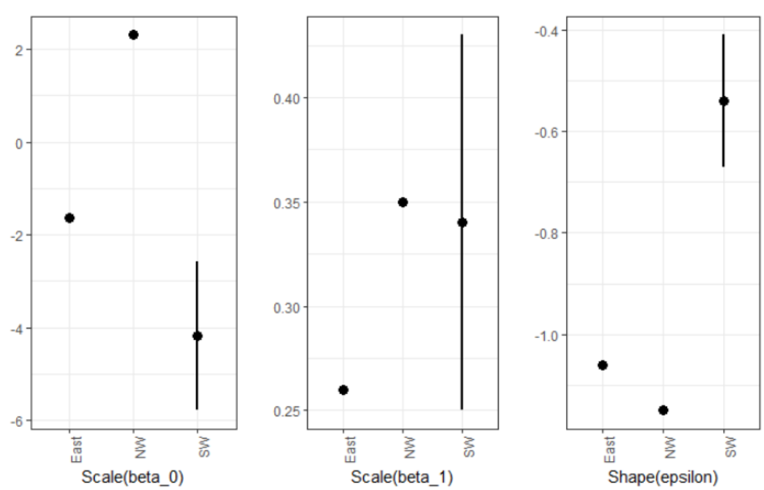

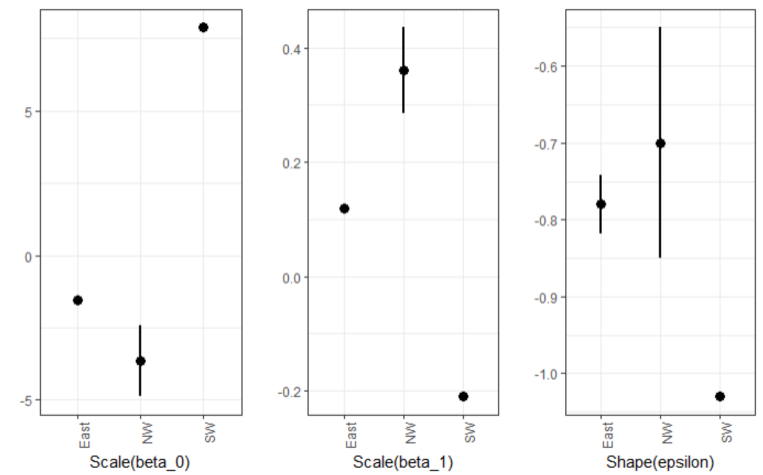

Figure 10: **Estimated parameters based on the best GPD model fitted to the winter minimum temperature in Southwest using Irkutsk data. Numerical values are listed in Table S.6.**

3.2.3 Results based on GEV and GPD models

In this section, we fitted the GEV and GPD distribution functions to the winter minimum temperature in Mongolia. The results are as follows:

- All the results show that the winter minimum temperature will follow the distributions with ε<0, namely the Weibull distribution for GEV and the upper-bounded Beta distribution.
- Based on BIC, GPD models show better performance in both Southwest and East regions, while the GED models show better performance in Northwest.

3.3 Return Periods of the Winter Minimum Temperature in Mongolia Simulated from Siberia Data

Next, we simulate the Mongolia winter minimum temperature based on data from Irkutsk Siberia for 197 years using the parameters estimated by the best GEV model. ~~We use the GEV model because the winter minimum temperature data is a single extreme value and that the GEV model is suitable for maxima and minima of block data.~~ Then, using this simulated Mongolia winter minimum temperatures, we estimate the 90% confidence intervals of return ~~levels~~periods of 10, 50 and 100 year events for each cluster (**Figure 11**~~**Figure 11**~~). The median of 100 year return ~~levels~~periods are -26.08, -27.99, and -

25.31 Celsius degrees for the Southwest, Northwest, and East. The variations in these density plots come from both the statistical properties of the Mongolia data itself and variations attributed to Siberia data.

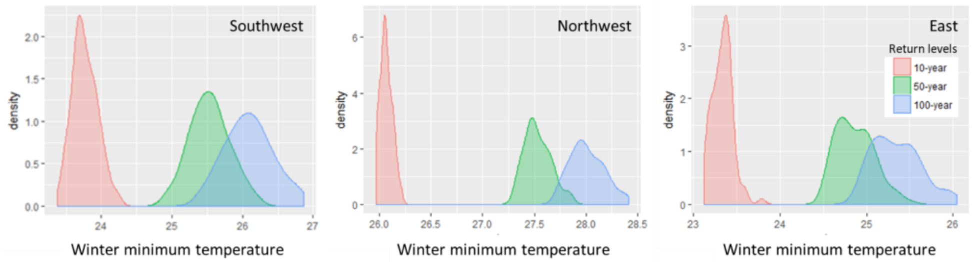

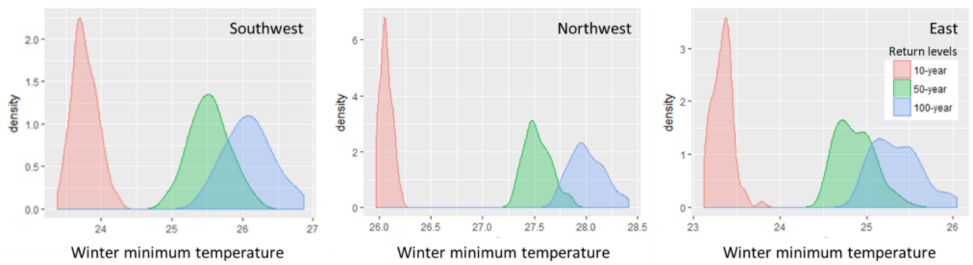

Figure 11: Density plots of 10, 50, and 100-year return ~~levels~~periods of the winter minimum temperatures in the Southwest, Northwest, and East of Mongolia with 90% confidence intervals. Please note that the x-axis shows temperature below zero (i.e., for Southwest, the axis shows negative 23.5 to 27 Celsius degree). The data is simulated 100 times from the Siberia data. For example, the plots show that the median of 100 year return ~~levels~~periods are -26.08, -27.99, and -25.31 Celsius degrees for the Southwest, Northwest, and East.

4. Binary Index

Based on the thresholds used in the GPD approaches, we also explored if the frequency of the co-occurrence of summer drought and cold winter temperatures has changed over time. First, we counted cases as a binary value of 1 when both summer drought and cold winter temperatures in Mongolia are below thresholds (-1 for PDSI values and -23 degree for winter temperatures), otherwise zero. Then, we fitted the local binomial and Poisson regressions while computing generalized cross-validation statistic to determine the smoothing parameter (Loader, 2006) (please see Section S.2 in the supplement for used alpha values for each cluster). Figure 12~~Figure 12~~ shows Northwest and East have similar long-term trends: decreasing trends in the early 20th century and the slightly increasing trends since 1990s. The Southwest shows an increase in the mid-20th century and has started happening again in the early 21st century.

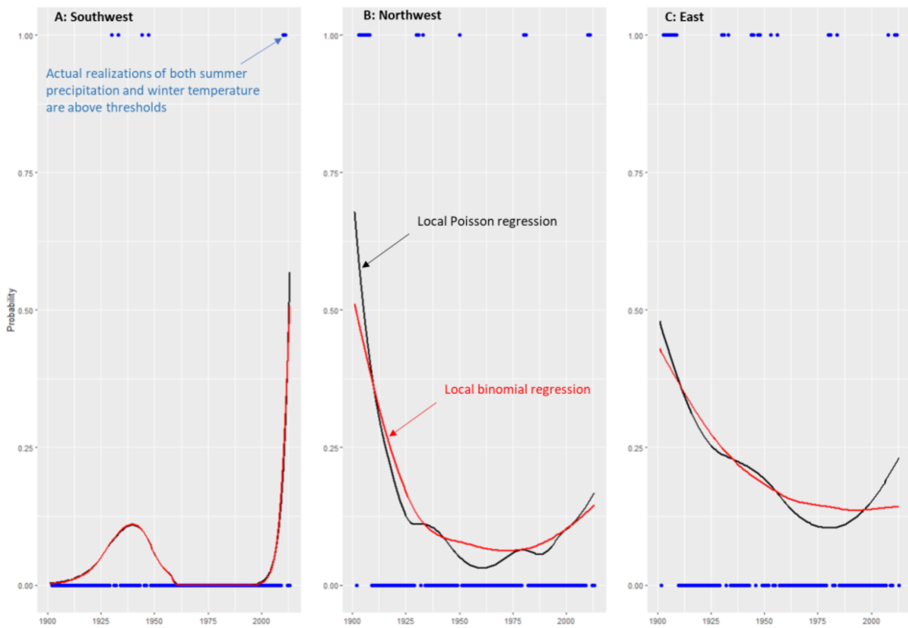

Figure 124: Binary index for the co-occurrence of threshold exceedance of PDSI values and winter temperature. The local regression is based on the optimal bandwidth of a local quadratic regression function based on the GCV criteria considering that the binary indicator is an outcome of a nonhomogeneous Poisson process. Note the tendency for a cluster in the beginning for the Northwest and the East. The increase in the frequency for the trend function in the most recent period could represent more of an edge effect of the regression.

5. Conclusions

Meteorological data in Mongolia is limited in length with many missing values. Therefore, we utilize longer records from paleoclimate proxy data and meteorological data from neighboring Siberia. ~~This study attempts~~The motivation was to improve risk estimation for dzud in Mongolia. Based on extreme value theory, this study derives fitted distributions for drought and winter extreme cold conditions. The study also improves the estimation of return periods of extreme drought conditions and winter temperature, using tree-ring reconstructed self-calibrated PDSI, and station records from Mongolia and Siberia.

GEV models without a threshold show that there is a ~~non-stationarity~~ trend in tree-ring reconstructed PDSI data in the Southwest, while there is a ~~stationarity~~no trend in PDSI in both the Northwest and East. However, the threshold approach indicates that extreme events in reconstructed PDSI values are stationary, indicating that catastrophic drought conditions ~~are~~were stationary for the last 300 years. si

The study estimated the extreme distributions of drought and winter minimum temperatures in Mongolia. The PDSI values follow the distributions with ε<0, namely the Weibull distribution for the GEV models and the upper-bounded Beta distribution for the GPD models. Also, the results of the study show that the winter minimum temperature follow the distributions with ε<0, namely the Weibull distribution for GEV and the upper-bounded Beta distribution. These estimated distributions can be used to improve the risk calculations for livestock index insurance in Mongolia.

Based on the results of our GEV fitted to the PDSI values, we show that climate variables, such as precipitation and snow, are important covariates for the extreme values of the reconstructed PDSI values. However, for catastrophic drought events, climate variables are not significant covariates based on the results of the GPD model fitted to the PDSI values.

The GEV model also shows that the return ~~levels~~periods of drought conditions are changing over time and variability is increasing for all the regions. Yet, based on GPD, the return ~~levels~~periods of drought conditions are constant: for example, the actual values of the PDSI for the 100-year events are: -4.17 for the Southwest, -4.76 for the Northwest, and -3.87 for the East. The median of 100-year return ~~levels~~periods of the winter minimum temperature in Mongolia is -26.08 Celsius degrees for the Southwest, -27.99 Celsius degrees for the Northwest, and -25.31 Celsius degrees for the East.

This study improves the return period estimation of droughts and winter minimum temperature. Summer drought and winter temperature are important predictors for livestock mortality since they explain 48.4% of the total variability in the mortality data, along with summer precipitation and summer potential evapotranspiration (Rao et al., 2015). Therefore, this long-term estimation of return periods of these significant predictors can be used to improve risk analysis of high livestock mortality in order to prepare for the winter catastrophes through early warning systems and index insurance.

A binary index for the co-occurrence of threshold exceedance of drought severity and temperature was developed and its temporal variation assessed. The index shows that all the regions have increasing trends of these co-occurrence. Begzsuren et al. (2004) identify that mortality rates are highest in combined drought and dzuds years than those with dzuds or drought alone while examining the co-occurrence of these extreme events with 51 years of observational data. This implies that the increasing trends of the co-occurrence would pose severe socioeconomic impacts on the country's livestock industry. (Rao et al., 2015) ~~Particularly~~

Our study estimates the return intervals and underlying probabilistic characteristics of the climate variables. Index insurance requires a proper threshold and the understanding of underlying distributions of risk events. Thus, the estimation of extreme value distributions and return ~~levels~~periods has the potential to improve livestock index insurance, which is implemented in

Mongolia by the Government of Mongolia with the help of the World Bank (Mahul et al., 2015)~~.~~. Insurance is priced by considering the uncertainty associated with the estimation of the probability of exceeding the threshold at which the pay-out occurs. The estimation of the uncertainty is reduced as the length of record (in our case from the paleoclimate extension) increases. At present, no one in the industry is using paleoclimatic information to extend and reduce coverage costs, but there is interest in using it to understand the clustering of pay-outs. Furthermore, the results of this study increase understanding of how extreme climatic events in arid regions, which are sensitive to anthropogenic climate change, are changing. The urgent needs to improve resilience of the society to this winter disaster is even more unequivocal.

Data Availability Statement

All relevant and publicly available data will be shared via a public data repository if the paper is accepted for publication; data sources are clearly specified throughout the paper.

Author contributions

MH, ND, MW, and UL designed the research. MH conducted data analysis. MR and CL prepared the dataset. MH prepared the manuscript with contributions and feedback from all co-authors.

Competing Interests

The authors declare that they have not conflict of interest.

Acknowledgements

ND and ~~MR~~MPR were supported by NSF OPP #1737788. MPR was also supported by the UCAR CPAESS NOAA Climate and Global Change Postdoctoral Fellowship under grant # NA18NWS4620043B. MW's work was supported by "Development of Innovative Green Technology and MRV Method for JCM (Joint Credit Mechanism) in Mongolia", which was funded by the Ministry of the Environment, Japan from 2014-2020~~.~~.

Reference

Mongolia: Severe Winter—Dzud. (Jun 2010) [dataset],
Mongolia : State of the Environment 2002.: http://www.rrcap.ait.asia/Publications/mongolia soe.pdf, last access: 8/25.
Akaike, H.: A Bayesian extension of the minimum AIC procedure of autoregressive model fitting, Biometrika, 66, 237-242, 1979.

Barnett, B. J. and Mahul, O.: Weather index insurance for agriculture and rural areas in lower-income countries, American Journal of Agricultural Economics, 89, 1241-1247, 2007.
Bat-Oyun, T., Shinoda, M., Cheng, Y., and Purevdorj, Y.: Effects of grazing and precipitation variability on vegetation dynamics in a Mongolian dry steppe, Journal of Plant Ecology, 9, 508-519, 2016.
Batima, P., Natsagdorj, L., Gombluudev, P., and Erdenetsetseg, B.: Observed climate change in Mongolia, Assess Imp Adapt Clim Change Work Pap, 12, 1-26, 2005.
Bayasgalan, B., Mijiddorj, R., Gombluudev, P., Oyunbaatar, D., Bayasgalan, M., Tas, A., Narantuya, T., and Molomjamts, L.: Climate change and sustainable livelihood of rural people in Mongolia, The adaptation continuum: groundwork for the future. ETC Foundation, Leusden, 193-213, 2009.
Begzsuren, S., Ellis, J. E., Ojima, D. S., Coughenour, M. B., and Chuluun, T.: Livestock responses to droughts and severe winter weather in the Gobi Three Beauty National Park, Mongolia, Journal of Arid environments, 59, 785-796, 2004.
Bell, A. R., Osgood, D. E., Cook, B. I., Anchukaitis, K. J., McCarney, G. R., Greene, A. M., Buckley, B. M., and Cook, E. R.: Paleoclimate histories improve access and sustainability in index insurance programs, Global environmental change, 23, 774-781, 2013.
Berger, J., Buuveibaatar, B., and Mishra, C.: Globalization of the cashmere market and the decline of large mammals in Central Asia, Conservation Biology, 27, 679-689, 2013.
Burnham, K. P. and Anderson, D. R.: Multimodel inference: understanding AIC and BIC in model selection, Sociological methods & research, 33, 261-304, 2004.
Cheng, L., AghaKouchak, A., Gilleland, E., and Katz, R. W.: Non-stationary extreme value analysis in a changing climate, Climatic change, 127, 353-369, 2014.
Cohen, J., Foster, J., Barlow, M., Saito, K., and Jones, J.: Winter 2009–2010: A case study of an extreme Arctic Oscillation event, Geophysical Research Letters, 37, 2010.
Coles, S., Bawa, J., Trenner, L., and Dorazio, P.: An introduction to statistical modeling of extreme values, Springer2001.
Cook, E. R., Anchukaitis, K. J., Buckley, B. M., D’Arrigo, R. D., Jacoby, G. C., and Wright, W. E.: Asian monsoon failure and megadrought during the last millennium, science, 328, 486-489, 2010.
D'Arrigo, R., Jacoby, G., Frank, D., Pederson, N., Cook, E., Buckley, B., Nachin, B., Mijiddorj, R., and Dugarjav, C.: 1738 years of Mongolian temperature variability inferred from a tree‐ring width chronology of Siberian pine, Geophysical Research Letters, 28, 543-546, 2001.
Dagvadorj, D., Natsagdorj, L., Dorjpurev, J., and Namkhainyam, B.: Mongolia assessment report on climate change 2009, Ministry of Nature, Environment and Tourism, Ulaanbaatar, 2, 34-46, 2009.
Dai, A., Trenberth, K. E., and Qian, T.: A global dataset of Palmer Drought Severity Index for 1870–2002: Relationship with soil moisture and effects of surface warming, Journal of Hydrometeorology, 5, 1117-1130, 2004.
Davi, N., Jacoby, G., Fang, K., Li, J., D'Arrigo, R., Baatarbileg, N., and Robinson, D.: Reconstructing drought variability for Mongolia based on a large‐scale tree ring network: 1520–1993, Journal of Geophysical Research: Atmospheres, 115, 2010.
Davi, N. K., D'Arrigo, R., Jacoby, G., Cook, E. R., Anchukaitis, K., Nachin, B., Rao, M. P., and Leland, C.: A long-term context (931–2005 CE) for rapid warming over Central Asia, Quaternary Science Reviews, 121, 89-97, 2015.
Davi, N. K., Rao, M., Wilson, R., Andreu‐Hayles, L., Oelkers, R., D’Arrigo, R., Nachin, B., Buckley, B., Pederson, N., and Leland, C.: Accelerated Recent Warming and Temperature Variability over the Past Eight Centuries in the Central Asian Altai from Blue Intensity in Tree Rings, Geophysical Research Letters, e2021GL092933, 2021.
Douglas A. Johnson, D. P. S., Daniel Miller and Daalkhaijav Damiran: Mongolian rangelands in transition, Sécheresse, 17, 133-141, 2006.
Fernandez-Gimenez, M. E., Batkhishig, B., and Batbuyan, B.: Cross-boundary and cross-level dynamics increase vulnerability to severe winter disasters (dzud) in Mongolia, Global Environmental Change, 22, 836-851, 2012.
Field, C. B.: Special Report on Managing the Risks of Extreme Events and Disasters to Advance Climate Change Adaptation: Summary for Policymakers: a Report of Working Groups I and II of the IPCC, Published for the Intergovernmental Panel on Climate Change2012.
Gao, J., Kirkby, M., and Holden, J.: The effect of interactions between rainfall patterns and land-cover change on flood peaks in upland peatlands, Journal of Hydrology, 567, 546-559, 2018.
Gilleland, E. and Katz, R. W.: extRemes 2.0: An extreme value analysis package in R, Journal of Statistical Software, 72, 1-39, 2016.
Harris, I., Jones, P. D., Osborn, T. J., and Lister, D. H.: Updated high‐resolution grids of monthly climatic observations–the CRU TS3.10 Dataset, International journal of climatology, 34, 623-642, 2014.
He, S., Gao, Y., Li, F., Wang, H., and He, Y.: Impact of Arctic Oscillation on the East Asian climate: A review, Earth-Science Reviews, 164, 48-62, 2017.
Hessl, A. E., Anchukaitis, K. J., Jelsema, C., Cook, B., Byambasuren, O., Leland, C., Nachin, B., Pederson, N., Tian, H., and Hayles, L. A.: Past and future drought in Mongolia, Science advances, 4, e1701832, 2018.
Hilker, T., Natsagdorj, E., Waring, R. H., Lyapustin, A., and Wang, Y.: Satellite observed widespread decline in Mongolian grasslands largely due to overgrazing, Global Change Biology, 20, 418-428, 2014.

Iijima, Y. and Hori, M. E.: Cold air formation and advection over Eurasia during “dzud” cold disaster winters in Mongolia, Natural Hazards, 92, 45-56, 2018.

Johnson, S. C.: Hierarchical clustering schemes, Psychometrika, 32, 241-254, 1967.

Kaheil, Y. and Lall, U.: Investigation of Climate Impact on Mongolian Livestock Mortality, 2011.

Kakinuma, K., Yanagawa, A., Sasaki, T., Rao, M. P., and Kanae, S.: Socio-ecological interactions in a changing climate: a review of the Mongolian pastoral system, Sustainability, 11, 5883, 2019.

Katz, R. W.: Statistics of extremes in climate change, Climatic change, 100, 71-76, 2010.

Katz, R. W.: Statistical methods for nonstationary extremes, in: Extremes in a changing climate, Springer, 15-37, 2013.

Katz, R. W., Parlange, M. B., and Naveau, P.: Statistics of extremes in hydrology, Advances in water resources, 25, 1287-1304, 2002.

Kendall, M. G.: Rank correlation methods, 1948.

Lall, U. and Kaheil, Y.: Investigation of climate imapct on mongolia livestock mortality, 2011.

Lall, U., Devineni, N., and Kaheil, Y.: An empirical, nonparametric simulator for multivariate random variables with differing marginal densities and nonlinear dependence with hydroclimatic applications, Risk Analysis, 36, 57-73, 2016.

Leonard, M., Westra, S., Phatak, A., Lambert, M., van den Hurk, B., McInnes, K., Risbey, J., Schuster, S., Jakob, D., and Stafford‐Smith, M.: A compound event framework for understanding extreme impacts, Wiley Interdisciplinary Reviews: Climate Change, 5, 113-128, 2014.

Liu, J., Hull, V., Batistella, M., DeFries, R., Dietz, T., Fu, F., Hertel, T. W., Izaurralde, R. C., Lambin, E. F., and Li, S.: Framing sustainability in a telecoupled world, Ecology and Society, 18, 2013.

Loader, C.: Local regression and likelihood, Springer Science & Business Media2006.

Mahul, O. and Skees, J. R.: Managing agricultural risk at the country level: The case of index-based livestock insurance in Mongolia, World Bank Policy Research Working Paper, 2007.

Mahul, O. and Stutley, C. J.: Government support to agricultural insurance: challenges and options for developing countries, World Bank Publications2010.

Mahul, O., Belete, N., and Goodland, A.: Innovations in insuring the poor: Index-based livestock insurance in Mongolia, 2015.

Mann, H. B.: Nonparametric tests against trend, Econometrica: Journal of the econometric society, 245-259, 1945.

McSharry, P.: The role of scientific modelling and insurance in providing innovative solutions for managing the risk of natural disasters, in: Reducing Disaster: Early Warning Systems For Climate Change, Springer, 325-338, 2014.

Middleton, N., Rueff, H., Sternberg, T., Batbuyan, B., and Thomas, D.: Explaining spatial variations in climate hazard impacts in western Mongolia, Landscape Ecology, 30, 91-107, 2015.

Minářová, J., Müller, M., Clappier, A., Hänsel, S., Hoy, A., Matschullat, J., and Kašpar, M.: Duration, rarity, affected area, and weather types associated with extreme precipitation in the Ore Mountains (Erzgebirge) region, Central Europe, International Journal of Climatology, 37, 4463-4477, 2017.

Morinaga, Y., Tian, S. F., and Shinoda, M.: Winter snow anomaly and atmospheric circulation in Mongolia, International Journal of Climatology: A Journal of the Royal Meteorological Society, 23, 1627-1636, 2003.

Munkhjargal, E., Shinoda, M., Iijima, Y., and Nandintseteseg, B.: Recently increased cold air outbreaks over Mongolia and their specific synoptic pattern, International Journal of Climatology, 40, 5502-5514, 2020.

Natsagdorj, L.: Some aspects of assessment of the dzud phenomena, Papers in Meteorology and Hydrology, 23, 3-18, 2001.

Palmer, W. C.: Meteorological drought (Vol. 30). Washington, DC, USA, US Department of Commerce, Weather Bureau, 1965.

Prosdocimi, I., Kjeldsen, T., and Miller, J.: Detection and attribution of urbanization effect on flood extremes using nonstationary flood‐frequency models, Water resources research, 51, 4244-4262, 2015.

Rao, M. P., Davi, N. K., D D’Arrigo, R., Skees, J., Nachin, B., Leland, C., Lyon, B., Wang, S.-Y., and Byambasuren, O.: Dzuds, droughts, and livestock mortality in Mongolia, Environmental Research Letters, 10, 074012, 2015.

Read, L. K. and Vogel, R. M.: Reliability, return periods, and risk under nonstationarity, Water Resources Research, 51, 6381-6398, 2015.

Reading, R. P., Bedunah, D. J., and Amgalanbaatar, S.: Conserving biodiversity on Mongolian rangelands: implications for protected area development and pastoral uses, In: Bedunah, Donald J., McArthur, E. Durant, and Fernandez-Gimenez, Maria, comps. 2006. Rangelands of Central Asia: Proceedings of the Conference on Transformations, Issues, and Future Challenges. 2004 January 27; Salt Lake City, UT. Proceeding RMRS-P-39. Fort Collins, CO: US Department of Agriculture, Forest Service, Rocky Mountain Research Station. p. 1-17,

Reynolds, J. F., Smith, D. M. S., Lambin, E. F., Turner, B., Mortimore, M., Batterbury, S. P., Downing, T. E., Dowlatabadi, H., Fernández, R. J., and Herrick, J. E.: Global desertification: building a science for dryland development, science, 316, 847-851, 2007.

Rootzén, H. and Katz, R. W.: Design life level: quantifying risk in a changing climate, Water Resources Research, 49, 5964-5972, 2013.

Salas, J. D. and Obeysekera, J.: Revisiting the concepts of return period and risk for nonstationary hydrologic extreme events, Journal of Hydrologic Engineering, 19, 554-568, 2014.

Skees, J. R. and Enkh-Amgalan, A.: Examining the feasibility of livestock insurance in Mongolia, World Bank Publications2002.

Slater, L. J., Anderson, B., Buechel, M., Dadson, S., Han, S., Harrigan, S., Kelder, T., Kowal, K., Lees, T., and Matthews, T.: Nonstationary weather and water extremes: a review of methods for their detection, attribution, and management, Hydrology and Earth System Sciences, 25, 3897-3935, 2021.
Tachiiri, K., Shinoda, M., Klinkenberg, B., and Morinaga, Y.: Assessing Mongolian snow disaster risk using livestock and satellite data, Journal of Arid Environments, 72, 2251-2263, 2008.
Van Buuren, S. and Groothuis-Oudshoorn, K.: mice: Multivariate imputation by chained equations in R, Journal of statistical software, 45, 1-67, 2011.
Willner, S. N., Levermann, A., Zhao, F., and Frieler, K.: Adaptation required to preserve future high-end river flood risk at present levels, Science advances, 4, eaao1914, 2018.
World Meteorological Organization: Climate Explorer [dataset],
Yu, Y., Ren, R., and Cai, M.: Comparison of the mass circulation and AO indices as indicators of cold air outbreaks in northern winter, Geophysical Research Letters, 42, 2442-2448, 2015.
Zscheischler, J., Martius, O., Westra, S., Bevacqua, E., Raymond, C., Horton, R. M., van den Hurk, B., AghaKouchak, A., Jézéquel, A., and Mahecha, M. D.: A typology of compound weather and climate events, Nature reviews earth & environment, 1, 333-347, 2020.

Supplement

S1: How to select a threshold for GPD.

To fit a GPD, a threshold needs to be selected. We selected the thresholds in the following ways. Figure S.3 repeatedly fits the GPD to the data for a series of threshold choices along with uncertainty (Gilleland and Katz, 2016). ~~Figure S.4~~Figure S.4 plots the mean excess values for a sequence of threshold choices with some variability information (Gilleland and Katz, 2016). As discussed in Gilleland and Katz (2016), choice of a threshold is subjective. Because a good choice of the threshold is near the inflection point of the right tail of the distribution, the value of 1.0 is selected as a threshold. This selection of 1 seems to yield estimates that will not change much as the threshold increases further from Figure S.3. Also, Gilleland and Katz (2016) suggests selecting a threshold whereby the graph is linear within uncertainty bounds in the plot of the mean excess values. Following this, the threshold value of 1 is a reasonable choice in Figure S.4. Furthermore, if I use this value for the threshold, the exceedance percentile of the threshold (a ratio of the number of exceedance to the number of total data) is 0.210 in the Southwest and 0.26 for both the northwest and east. These thresholds correspond to 4-5 years return periods. Setting these return levels as thresholds is of interest in terms of social concern. Therefore, it is reasonable to use a threshold of 1.0. In the same way, the threshold value of minus 23 degree is selected for the winter temperature Figure S.5 and Figure S.6, corresponding the 4-5 years return periods.

S2: Local regression in Section 5

Please note that local Poisson regressions for the Southwest use alpha=0.5, for the Northwest alpha=0.5, and the East alpha=0.65 for smoothing parameters respectively. Local binomial regressions for the Southwest use alpha=0.5, for the Northwest alpha=0.8, and for East alpha=0.9. All are a 1 degree of freedom.

S3: Figures

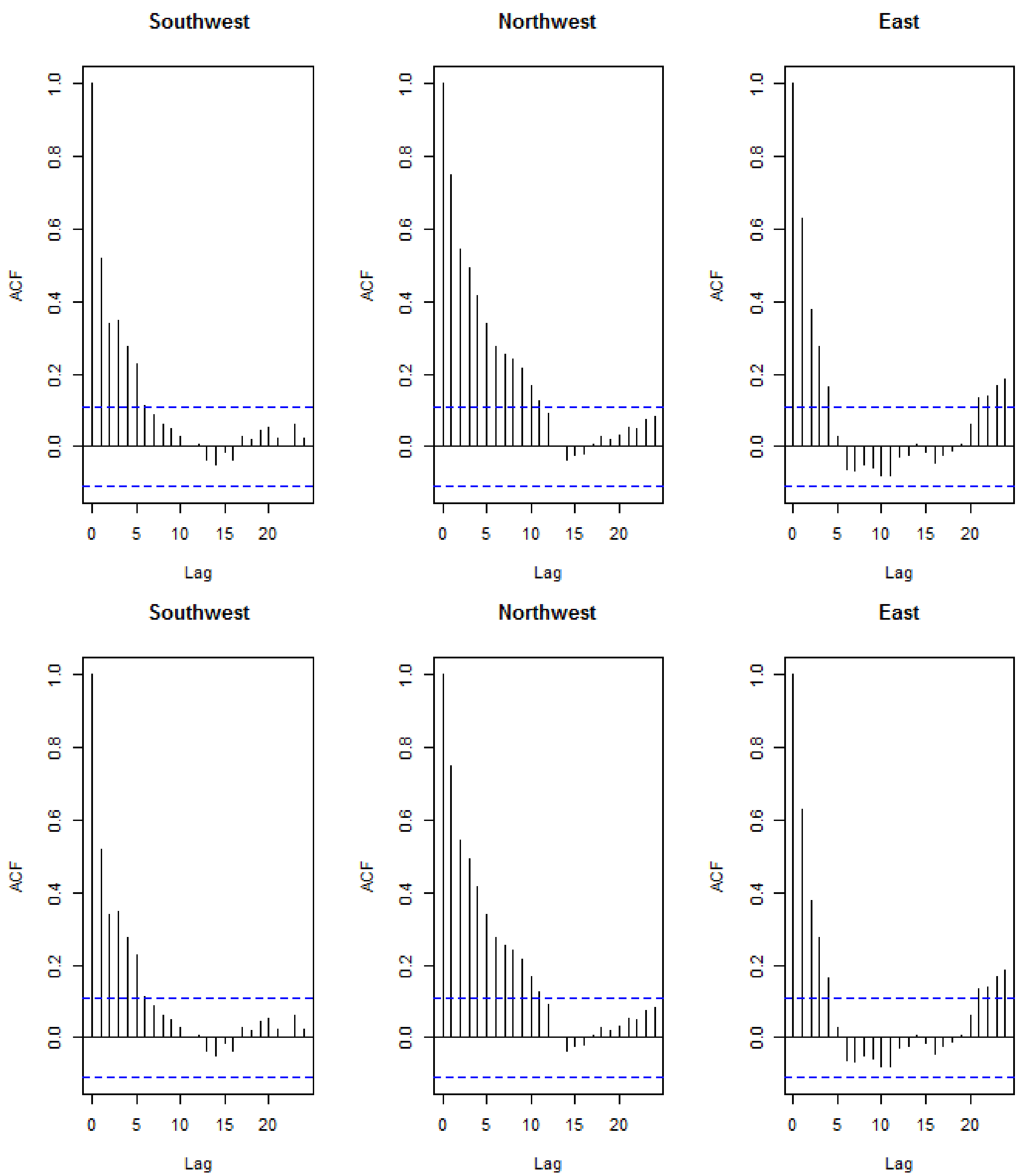

Figure S.1: ACF of the tree-ring reconstructed PDSI in each cluster.

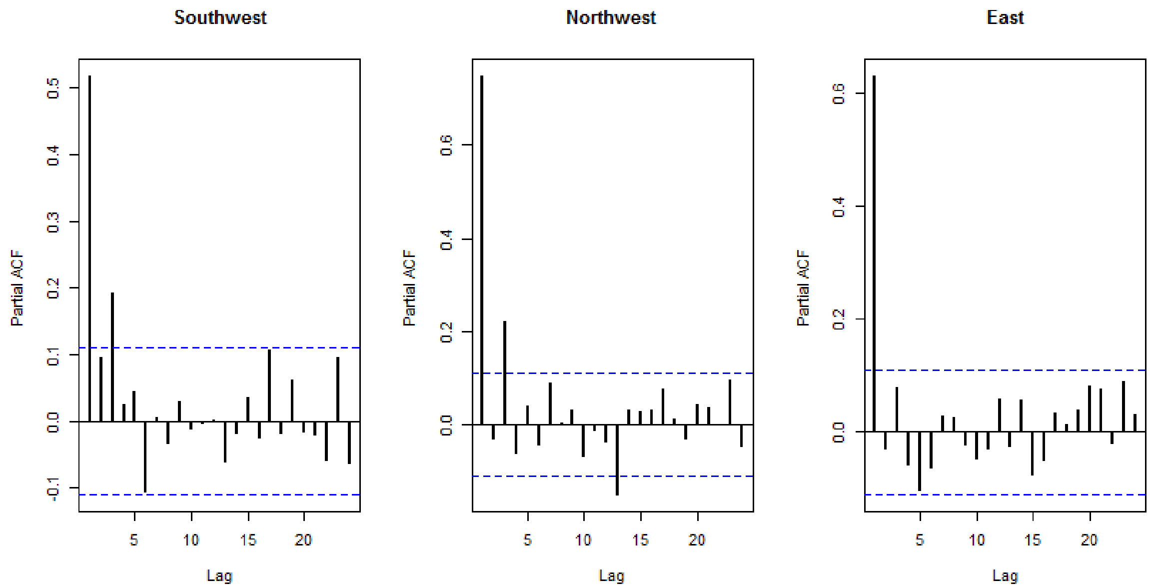

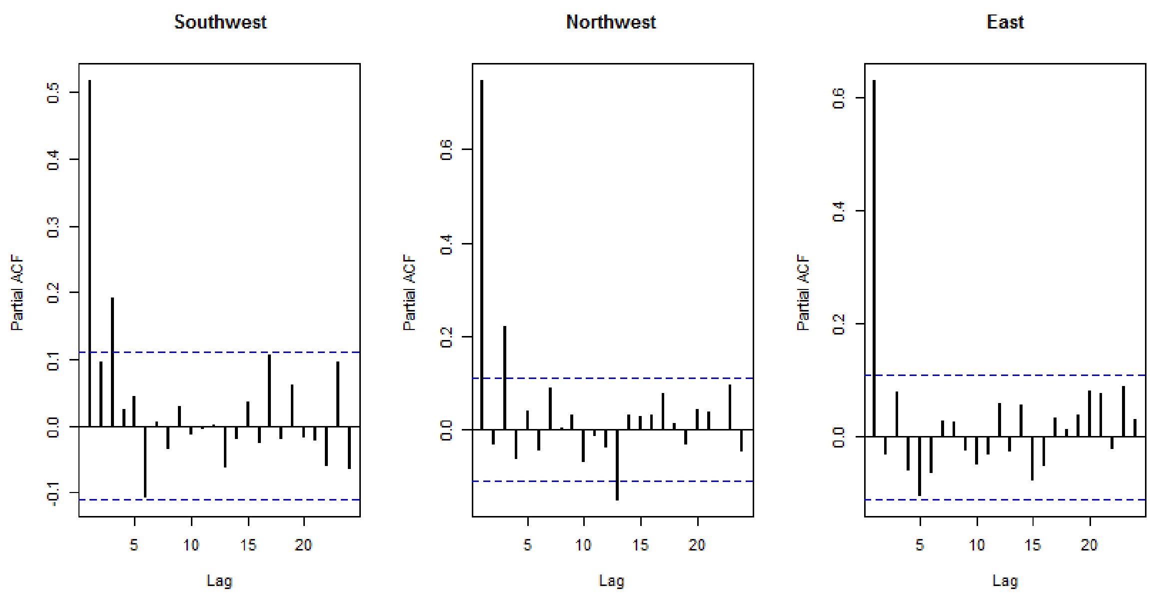

Figure S.2: PACF of the tree-ring reconstructed PDSI in each cluster.

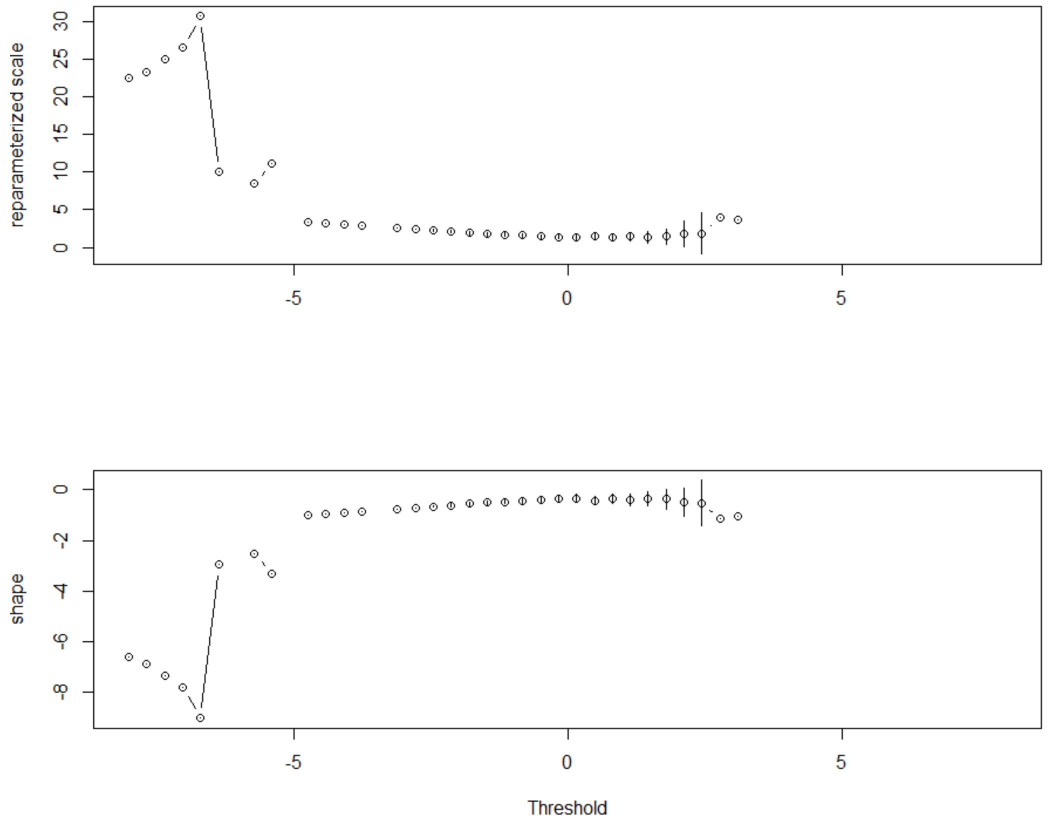

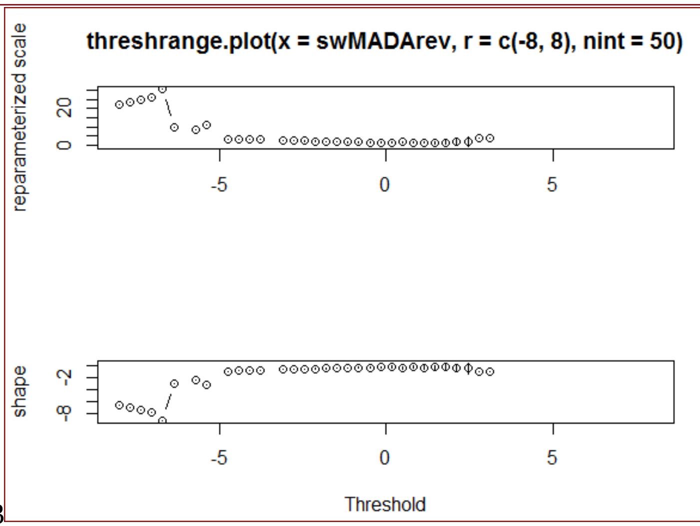

Figure S.3

~~Figure S.: Threshold Range Plot (1)~~

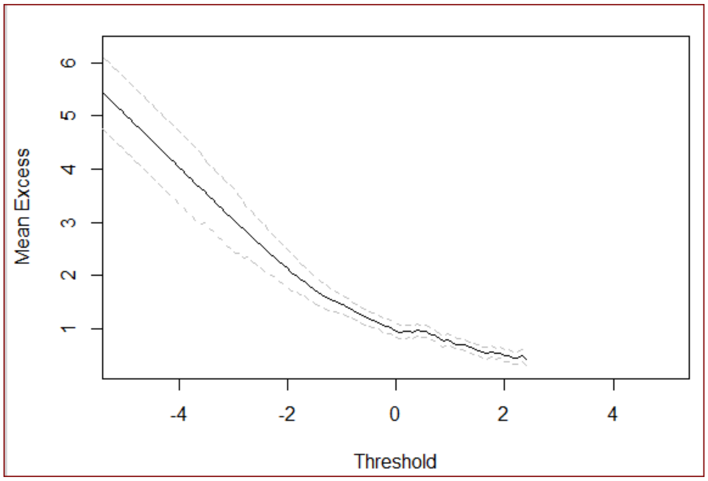

: Threshold Range Plot. This figure is used to choose a threshold for GPD following Gilleland and Katz (2016). The figure repeatedly fits the GP distribution function to the data to plot a sequence of threshold choices with some variability information. A subjective selection of 1 as a threshold appears to yield estimates that will not change much. Also, this selection is made based on Fig S4 and the theoretical and practical justification (which means that a threshold of 1 corresponds to a 4- 5 year return level, which is of social interests.) Reparametarization means here the scale parameter is adjusted so that it is not a function of threshold (Gilleland and Katz (2016)).

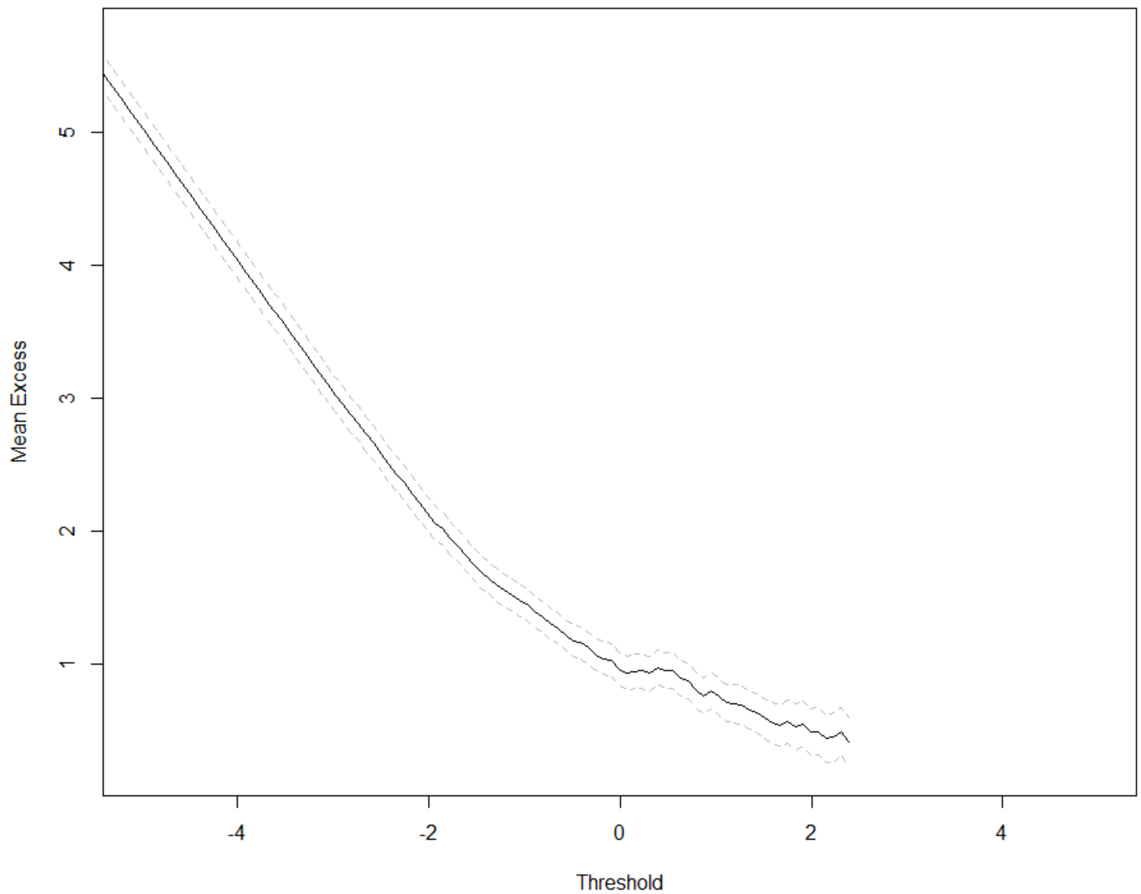

Figure S.4: Empirical mean residual life plot to determine a threshold range of PDSI value in the Southwest. The inflection point is shown around 0-1. We subjectively select 1 as explained in Gilleland and Katz (2016).

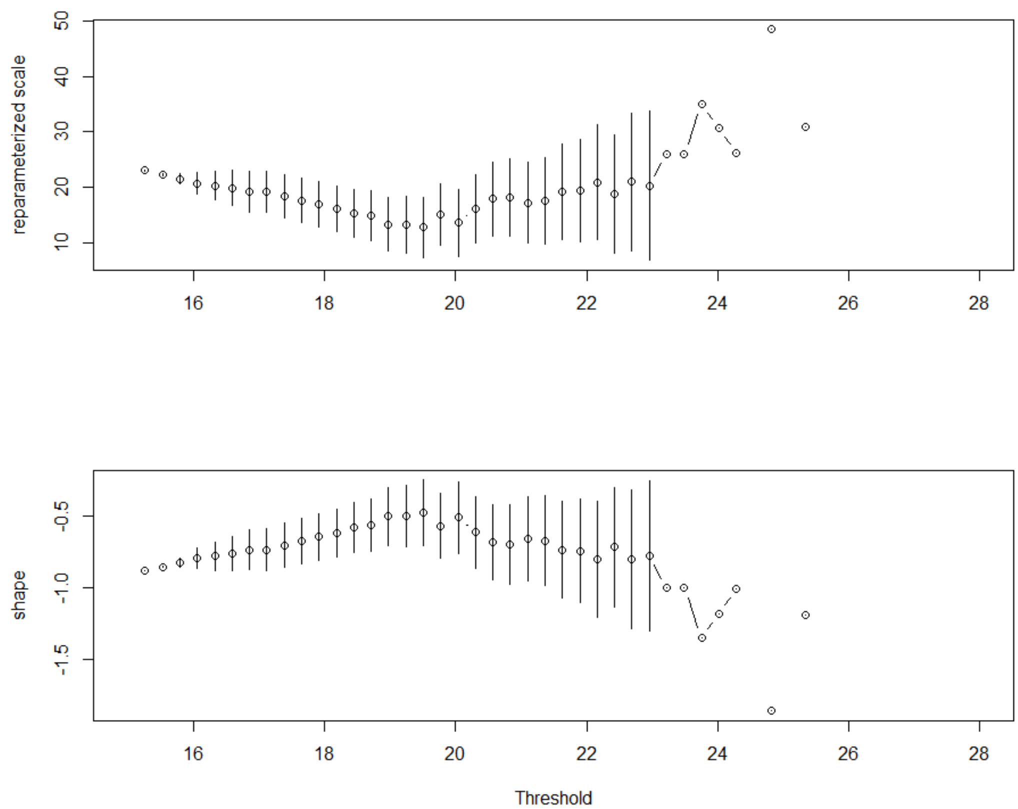

Figure S.5: Threshold range plot ~~(2)~~of temperature in southwest. This figure is used to choose a threshold for GPD following Gilleland and Katz (2016).

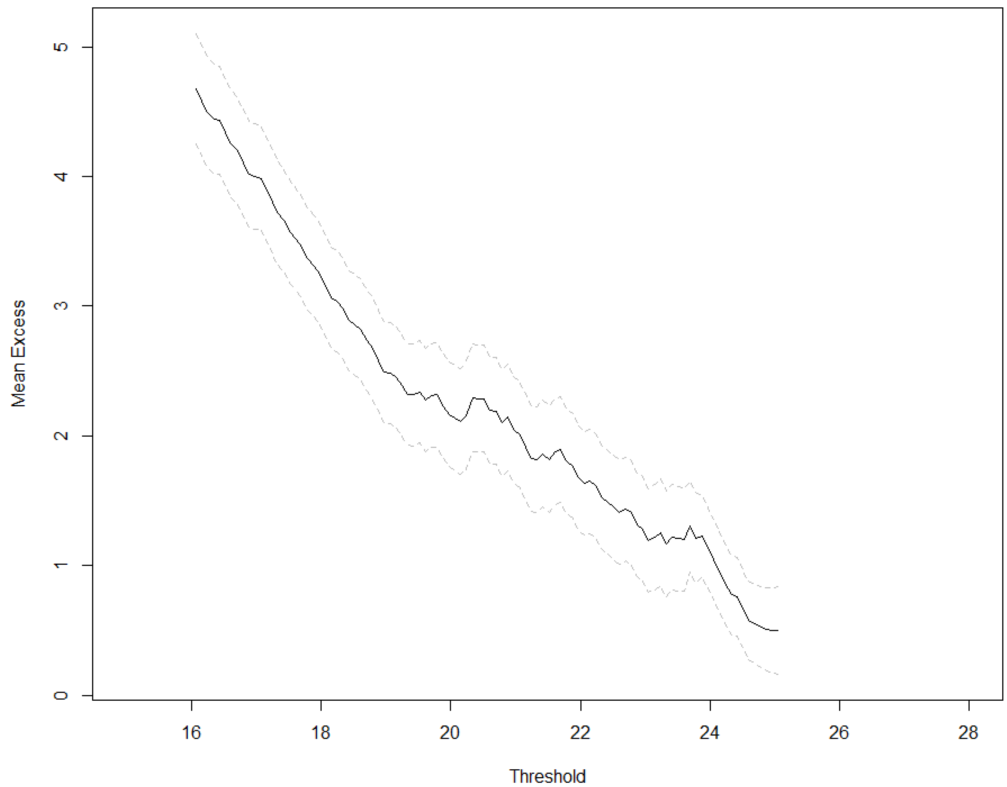

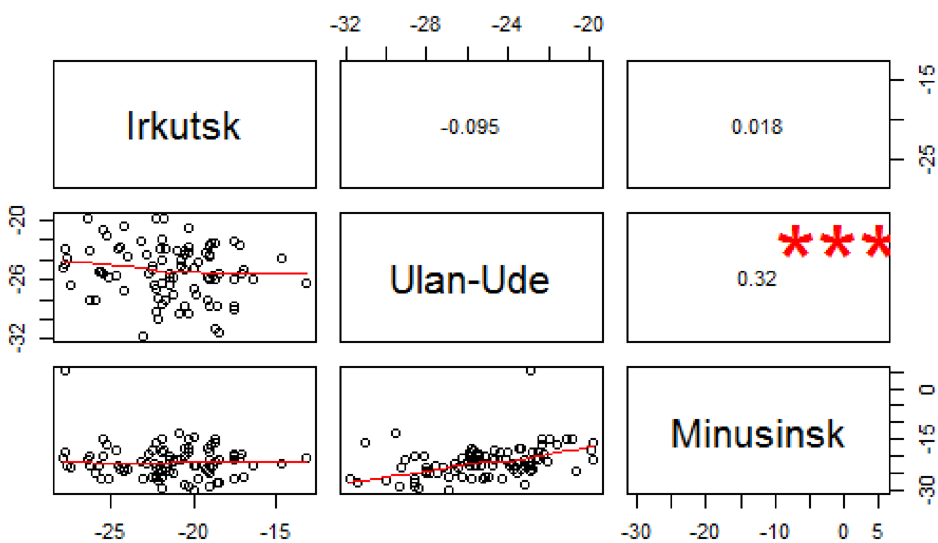

Figure S.6

~~Figure S.~~: Empirical mean residual life plot to determine threshold range of temperature in southwest. The inflection point is shown around 23. We subjectively select 23 as explained in Gilleland and Katz (2016).

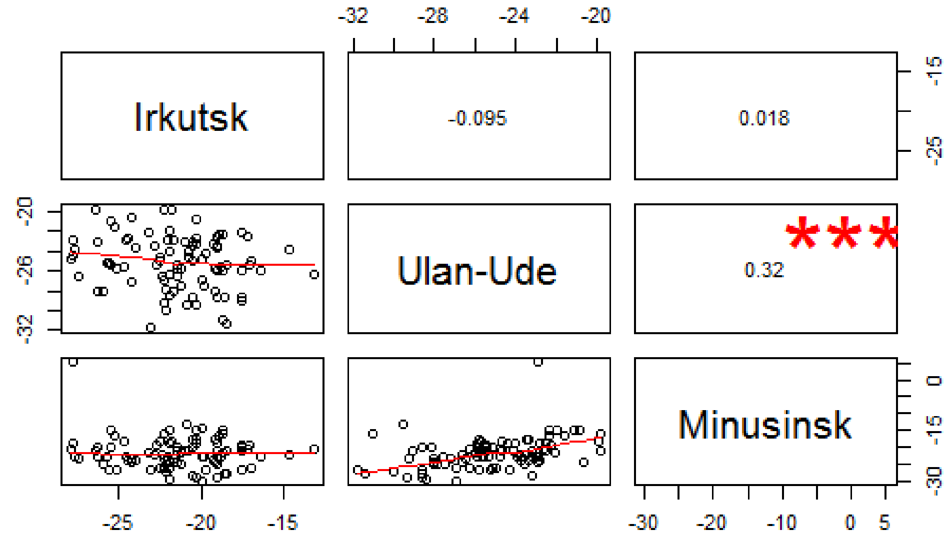

Figure S.7: Scatterplots between winter minimum temperature in three Siberia stations. Red marks show statistical significance, while red curves show the smoothed curve. One, two or three stars indicate that the corresponding variable is significant at 10%, 5% and 1% levels, respectively.

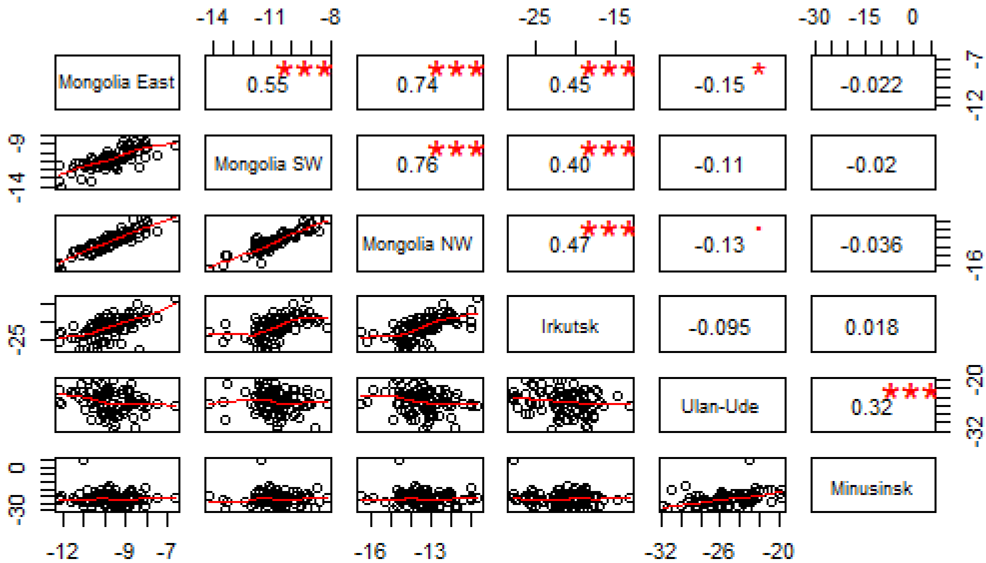

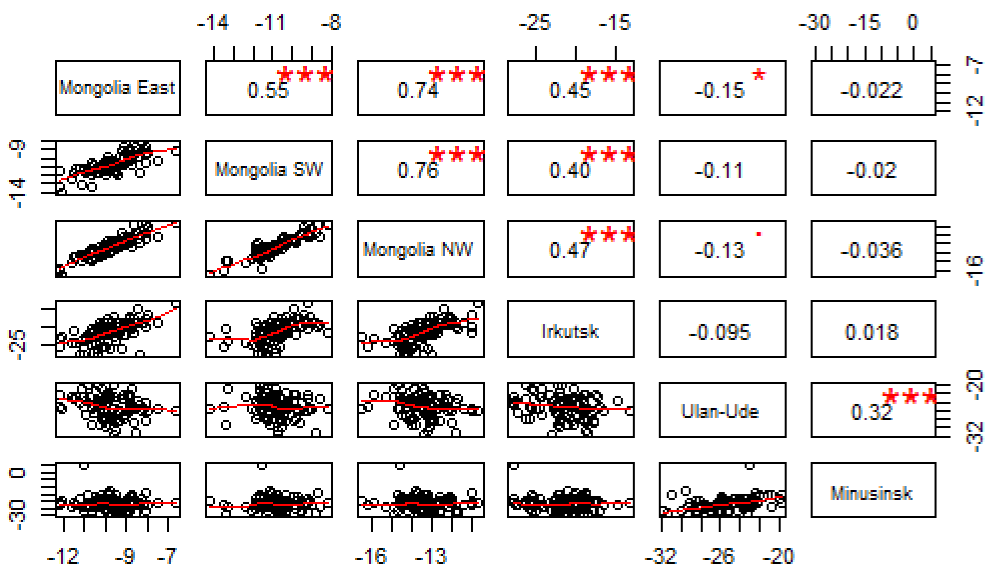

Figure S.8: Scatterplots of winter average temperature in three Siberia and three Mongolia clusters. **One, two or three stars indicate that the corresponding variable is significant at 10%, 5% and 1% levels, respectively.**

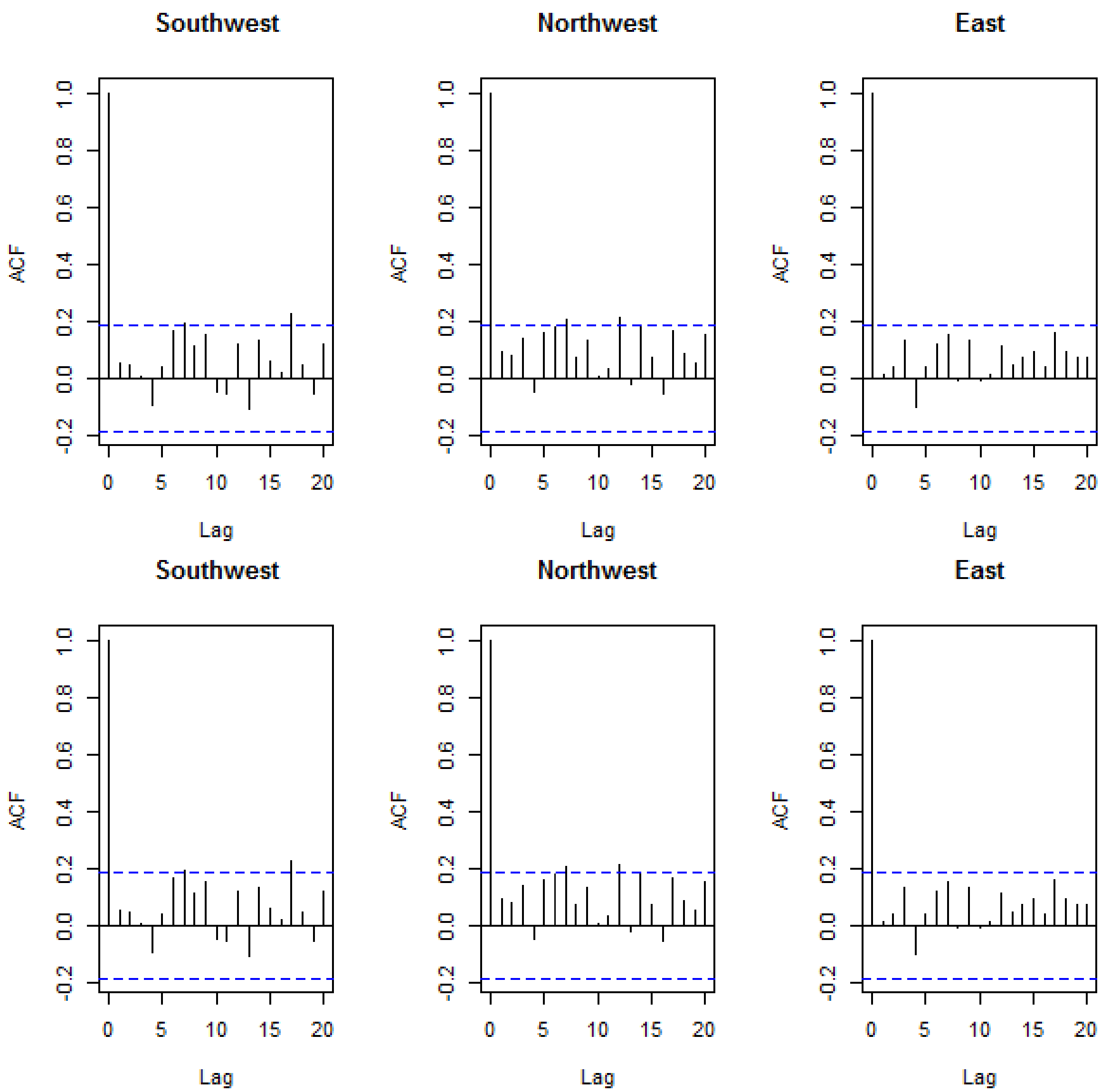

Figure S.9: ACF of residuals between data from Irkutsk Siberia and the winter average temperature of each cluster.

A.3: Tables

Table S.1: 95% Confidence intervals of parameters based on the normal approximation for each region.

	95% lower CI	Estimate	95% upper CI
Southwest			
Location (α_0)	-0.56	-0.42	-0.28
Scale (β_0)	0.75	0.95	1.15
Scale (β_1)	0.001	0.002	0.003
Shape (ε)	-0.29	-0.23	-0.17
Northwest			
Location(α_0)	-0.87	-0.67	-0.46

Scale (β_0)	1.53	1.68	1.82
Shape (ε)	-0.32	-0.25	-0.18
East			
Location(α_0)	-0.93	-0.73	-0.52
Scale (β_0)	1.51	1.65	1.80
Shape (ε)	-0.38	-0.31	-0.24

Table S.2: 95% Confidence intervals of parameters, using other climate variables based on the normal approximation

	95% lower CI	Estimates	95% Upper CI
Southwest			
Location (α_0)	2.49	3.63	4.77
Location (β_1)	-0.18	-0.14	-0.11
Scale (β_0)	0.96	1.12	1.28
Shape(ε)	-0.33	-0.21	-0.10
Northwest			
Location (α_0)	4.84	6.25	7.67
Location (α_1)	-0.17	-0.15	-0.12
Scale (β_0)	1.60	2.38	3.17
Scale (β_1)	-0.48	-0.31	-0.14
Shape (ε)	-0.20	-0.07	0.06
East			
Location (α_0)	3.01	5.09	7.17
Location (β_1)	-0.17	-0.13	-0.08
Scale (β_0)	1.26	1.48	1.71
Shape (ε)	-0.39	-0.24	-0.10

Table S.3: 95% Confidence intervals of parameters, using other climate variables based on the normal approximation

	95% lower CI	Estimate	95% upper CI
Southwest			
Scale (β_0)	0.33	0.78	1.24
Shape (ε)	-0.64	-0.20	0.22
Northwest			
Scale (β_0)	0.78	2.02	3.25
Shape(ε)	-1.01	-0.53	-0.05
East			
Scale(β_0)	0.85	1.88	2.91
Shape(ε)	-1.13	-0.65	-0.18

Table S.4: Pearson and Spearman correlation coefficients in winter minimum temperature between Mongolia data and Siberia data

	Southwest	Northwest	East
Pearson correlation coefficients			
Irkutsk, Siberia	0.57***	0.72***	0.76***
Ulan-Ude, Siberia	-0.14	-0.13	-0.21*

Minusinsk, Siberia	-0.04	-0.09	-0.16
Spearman correlation coefficients			
Irkutsk, Siberia	0.52***	0.61***	0.60***
Ulan-Ude, Siberia	-0.14	-0.19	-0.22*
Minusinsk, Siberia	-0.02	-0.08	-0.08

Note: One, two or three stars indicate that the corresponding variable is significant at 10%, 5% and 1% levels, respectively.

Table S.5: Estimated parameters based on the best GEV model fitted to the winter minimum temperature in Southwest using Irkutsk data.

	Estimate	Standard Error Estimates
Southwest		
Location (α_0)	11.82	1.22
Location (α_1)	0.39	0.06
Scale (β_0)	1.90	0.14
Shape (ε)	-0.25	0.06
Northwest		
Location (α_0)	12.67	1.00
Location (α_1)	0.52	0.05
Scale (β_0)	0.35	0.66
Scale (β_1)	0.06	0.03
Shape	-0.18	0.06
East		
Location (α_0)	10.20	0.80
Location (α_1)	0.48	0.04
Scale (β_0)	1.40	0.10
Shape (ε)	-0.38	0.05

Table S.6: Estimated parameters based on the best GPD model fitted to the winter minimum temperature in Southwest using Irkutsk data.

	Estimate	Standard Error Estimates
Southwest		
Scale (α_0)	~~-4.18~~7.87	2e-08~~1.60~~
Scale (α_1)	-0.~~34~~21	2e-08~~0.09~~
Shape	~~-0.54~~1.03	2e-08~~0.13~~
Northwest		
Scale(β_3)	~~2.30~~-3.66	1.22~~2e-08~~
Scale (β_4)	0.~~35~~36	0.075~~2e-08~~
Shape	~~-1.15~~0.70	0.15~~2e-08~~
East		
Scale	-1.~~63~~55	2e-08
Scale (β_4)	0.~~26~~12	2e-08
Shape	~~-1.06~~0.78	~~2e-08~~0.038